Ecole Nationale de Biologie Structurale Intégrative

1-6 Juin 2014 – Oléron, France

Nuclear Magnetic Resonance – Conceptual aspects

NMR observables:
A source of structural and dynamical information for the study of biomacromolecules

Catherine Bougault, IBS, Grenoble

catherine.bougault@ibs.fr

Curriculum

1991-1994 PhD in Inorganic Chemistry (CEA Grenoble, France)
« New asymetric iron-sulfur clusters with cyclotriveratrylenic thiolate ligands : synthesis and spectroscopic characterizations »

1995 Postdoctoral position at UC Davis, USA, with G. N. La Mar
« Electronic states of high-spin deoxymyoglobin »

1996 Assistant professor in L.E.D.S.S. at Joseph Fourier University
Paramagnetic NMR of small molecules

2001-2003 Visiting scientist at University of Georgia, Athens, with J. H. Prestegard
Thermostability of rubredoxin

Since 2003 Assistant professor at Joseph Fourier University
Research in the biomolecular NMR spectroscopy group at IBS
Bacterial cell wall and antibiotic resistance

NMR : a structural biology tool among others

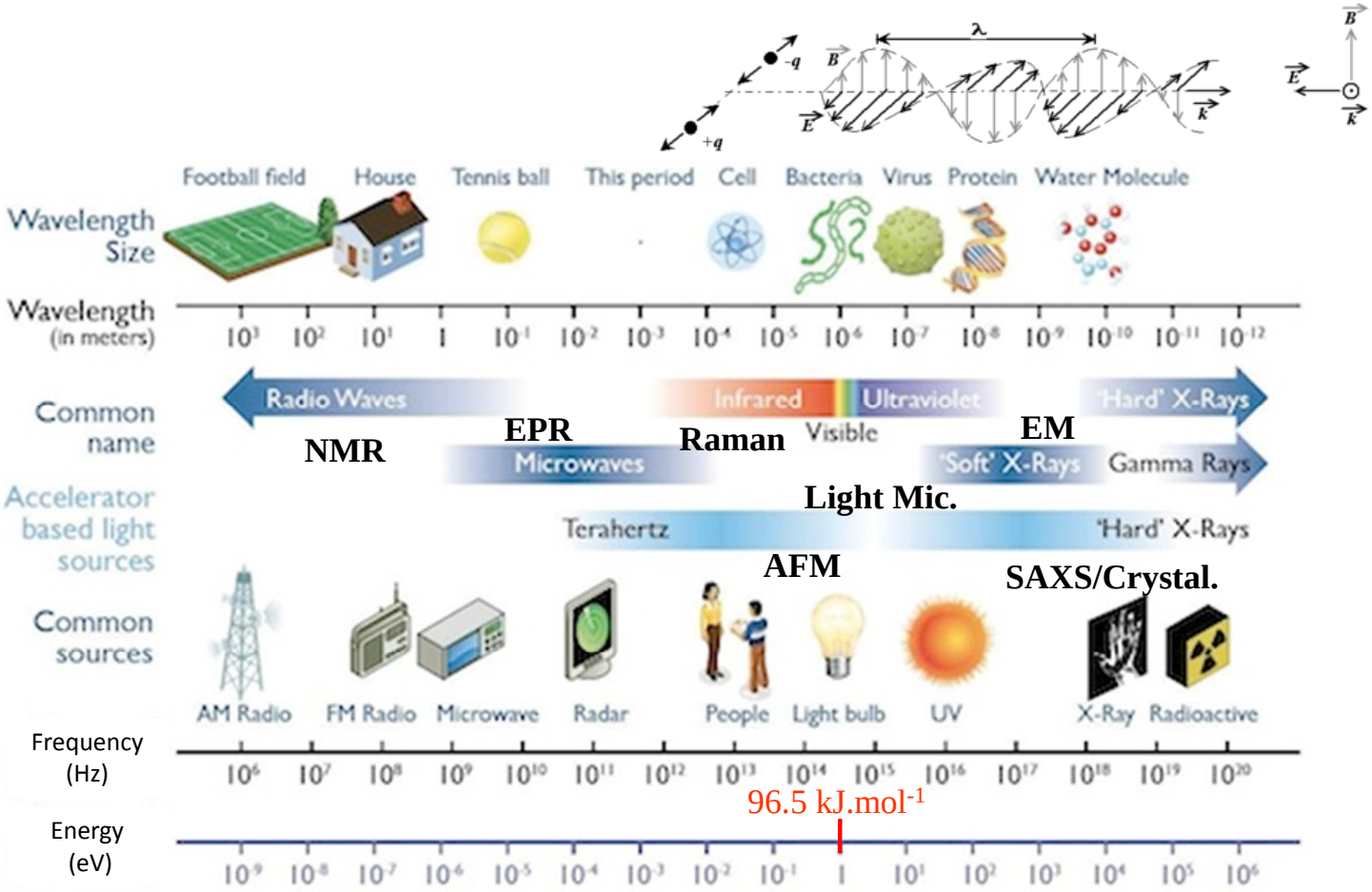

www.lightsources.org/what-light-source

X-ray: from the sample to the 3D structure

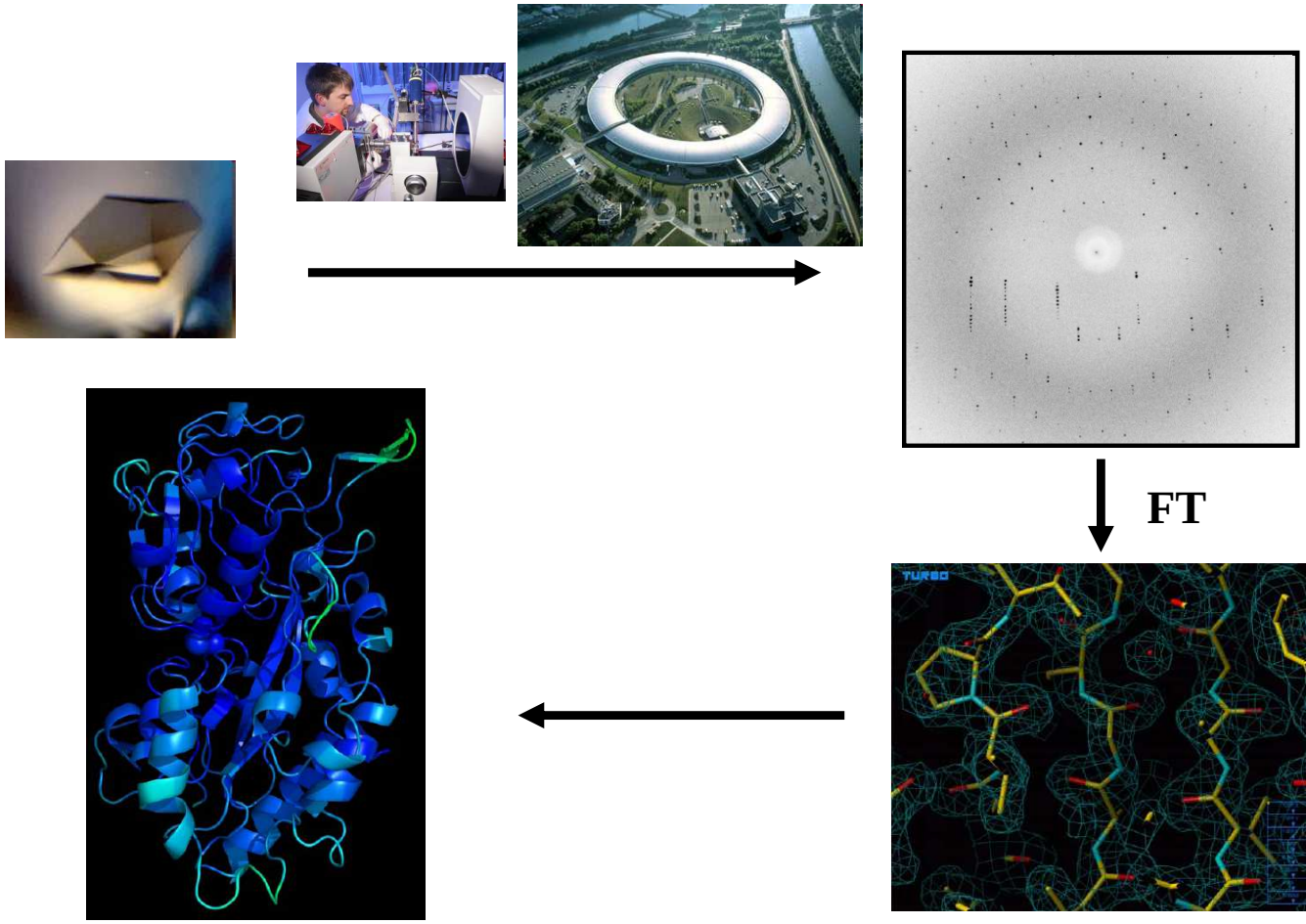

NMR: from the sample to the 3D structure

FT

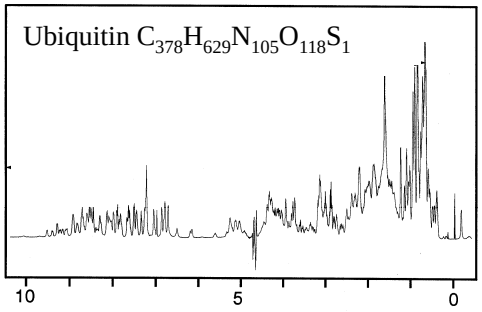

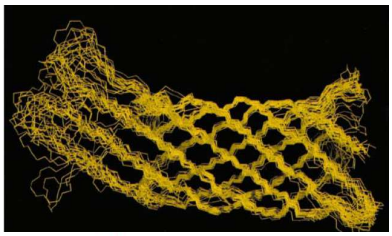

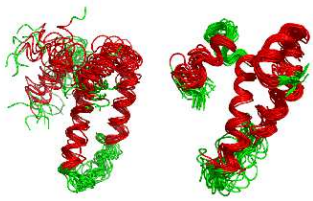

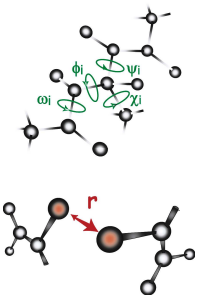

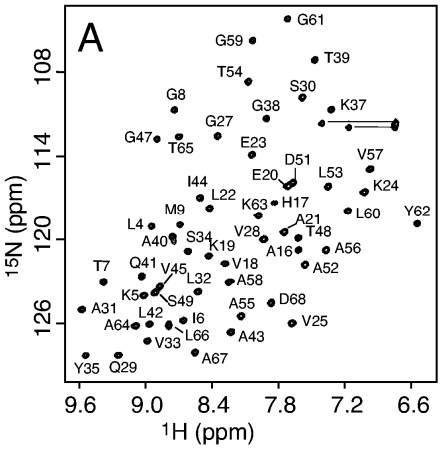

NMR : a structural biology tool among others

	Proteins	Nucleic Acids	Protein/ NA Complex	Other	Total
X-Ray	83194	1522	4342	4	89062
NMR	**9176**	**1082**	**210**	**7**	**10475**
Electron Microscopy	540	54	173	0	767
Other	155	4	6	13	65
Total	**93124**	**2665**	**4733**	**25**	**100547**

Protein Data Bank: May 31st, 2014 statistics

http://www.rcsb.org

PDB Statistics

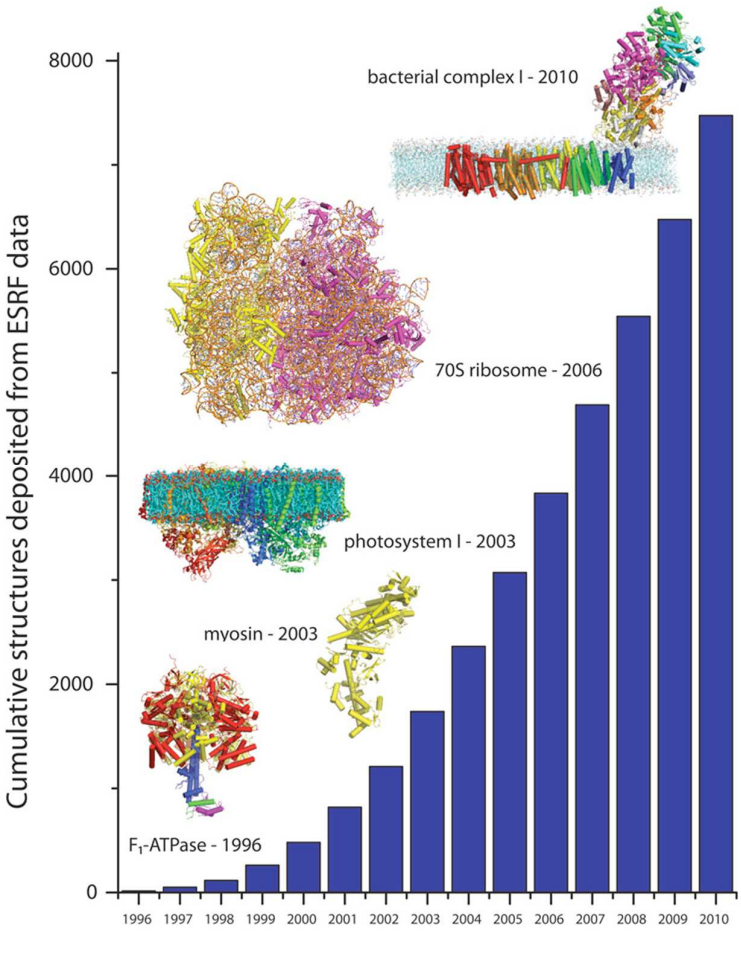

NMR: developments and limits

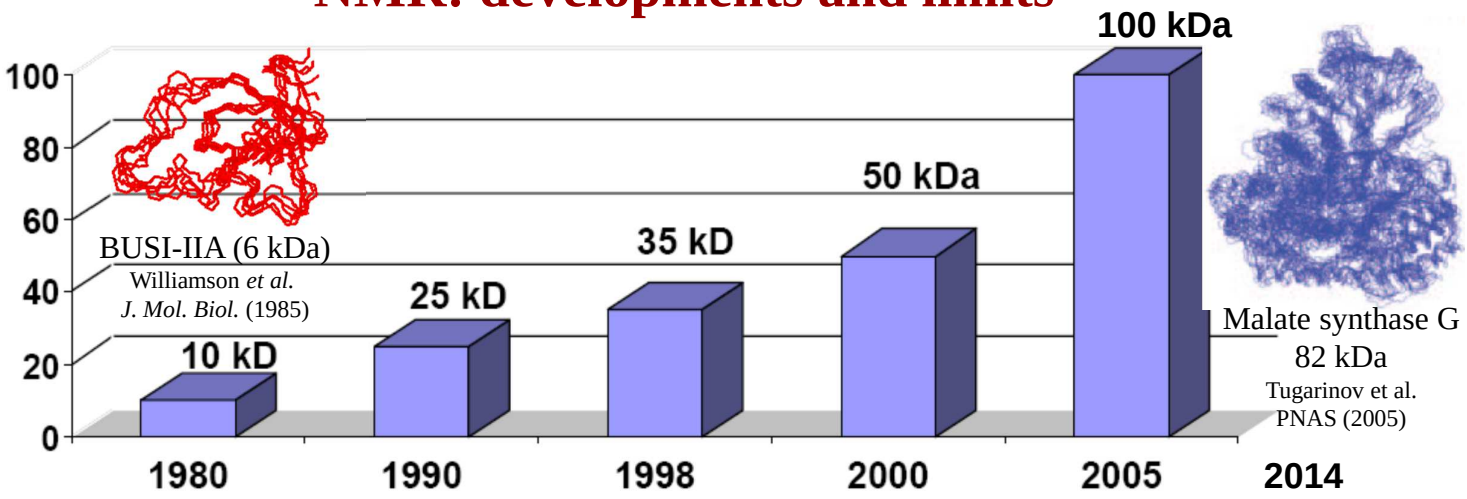

Magnets	500 MHz	600 MHz	800 MHz	900 MHz	950 MHz	1.2 GHz
Cryoprobes				500, 600	700,800	1000
Sequences	2D	3D, 4D Triple resonance Gradients	TROSY			
Constraints	NOE			RDC, CCR		
Labeling	none	^{13}C, ^{15}N	^{2}H, ^{13}C,^{15}N		specific labeling	

NMR: developments and limits

Liquid-state NMR a serious limit?

Linewidth

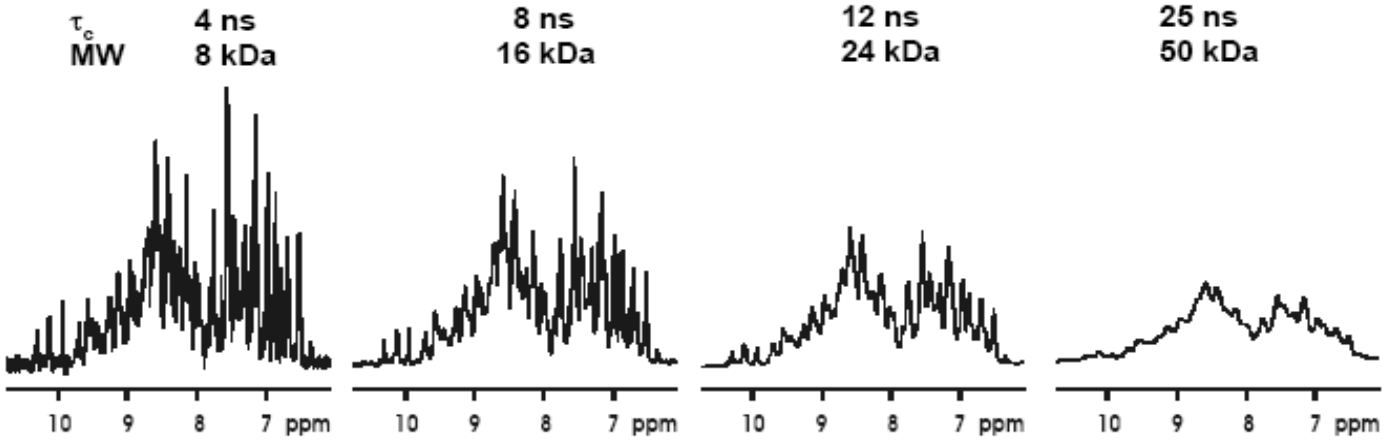

fast overall rotation

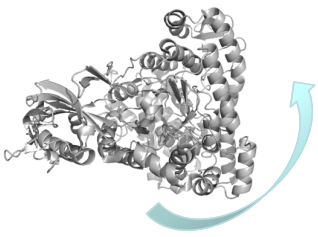

slow overall rotation

NMR: developments and limits

Trying to overcome liquid-state NMR limits – Strategy 1

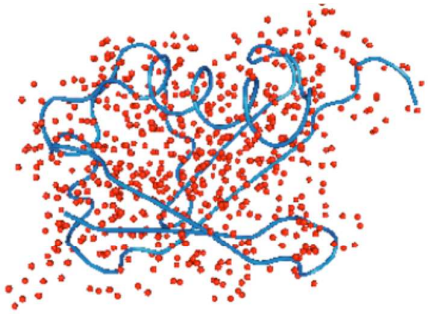

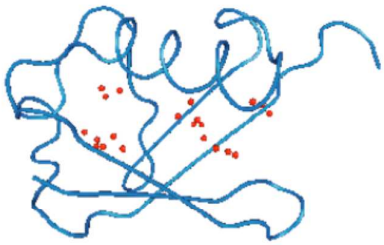

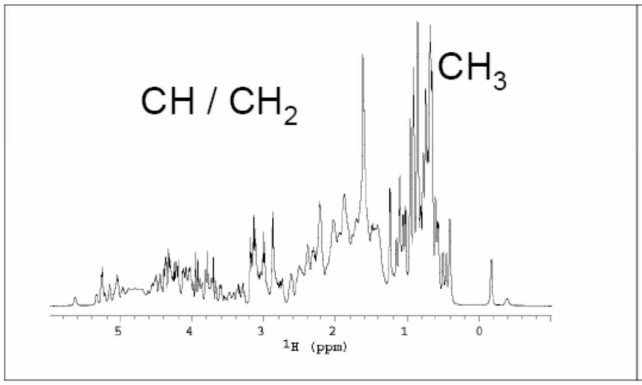

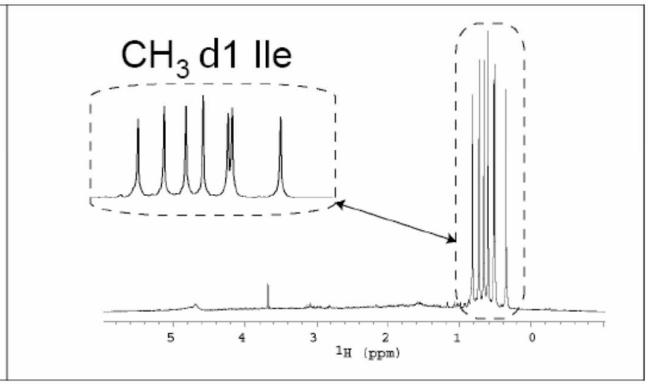

^{1}H ubiquitin in H_2O

U-[^{2}H, ^{15}N], δ_1[^{1}H, ^{13}C]-CH_3-ubiquitin in H_2O

NMR: developments and limits

TET-2 468 kDa, homododecamer

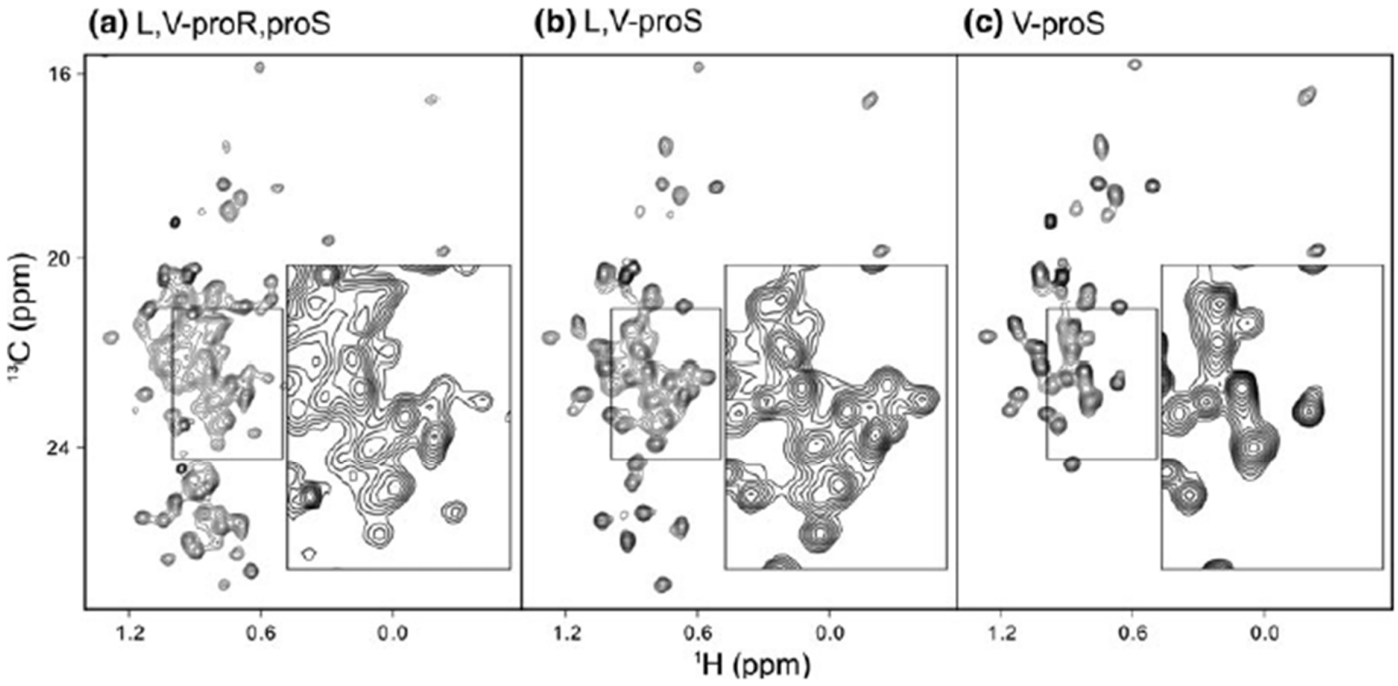

α-spectrin SH3 domain – INEPT or CP transfer – MAS 24 kHz
G mAs, E Crublet, O Hamelin, P Gans, J Boisbouvier, *J. Biomol. NMR*, **2013**, 57), pp 251-262

NMR: developments and limits

Trying to overcome liquid-state NMR limits – Strategy 2

Liquid-state NMR

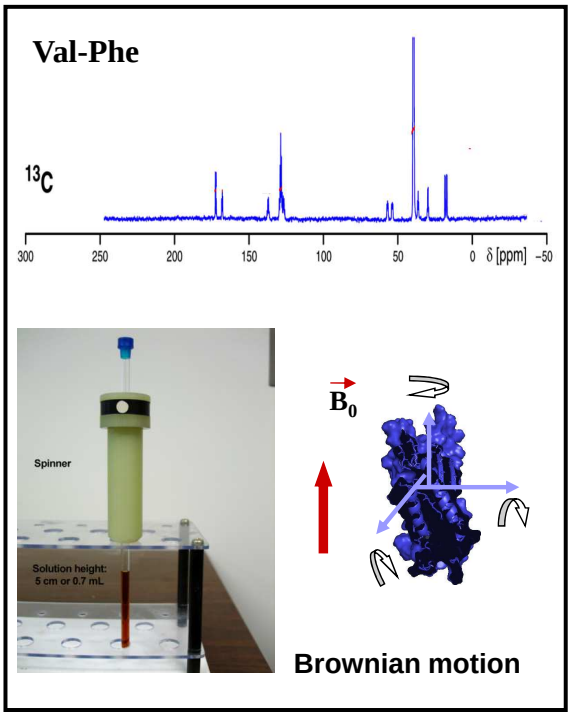

~ 400 µL of soluble sample

Solid-state NMR

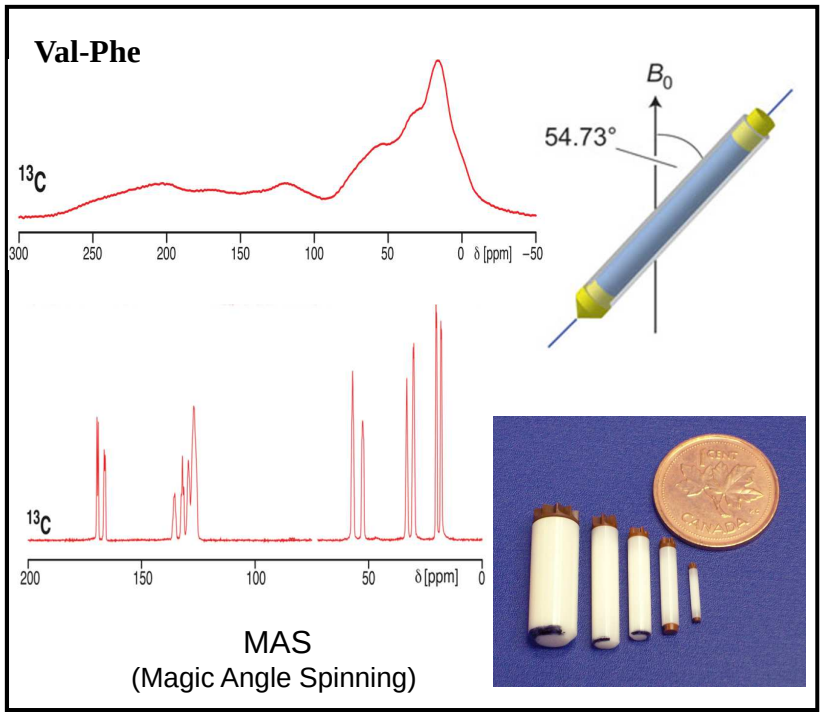

~ 20 mg of microcrystals

NMR: developments and limits

Trying to overcome liquid-state NMR limits

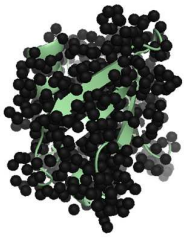

^{15}N-ubiquitin

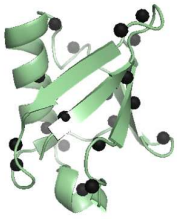

[^{2}H, ^{15}N]-ubiquitin 70-90% D_2O

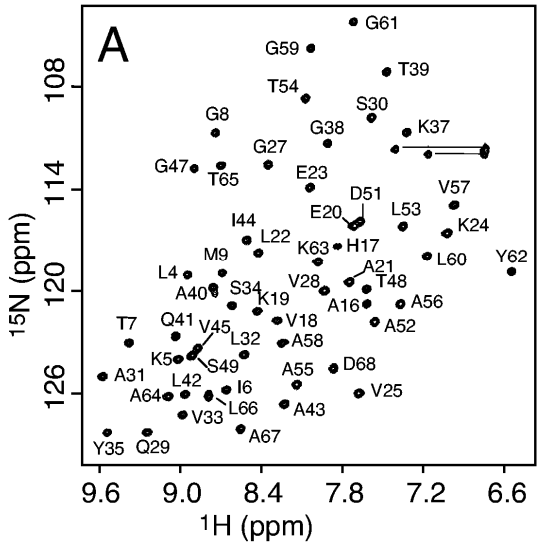

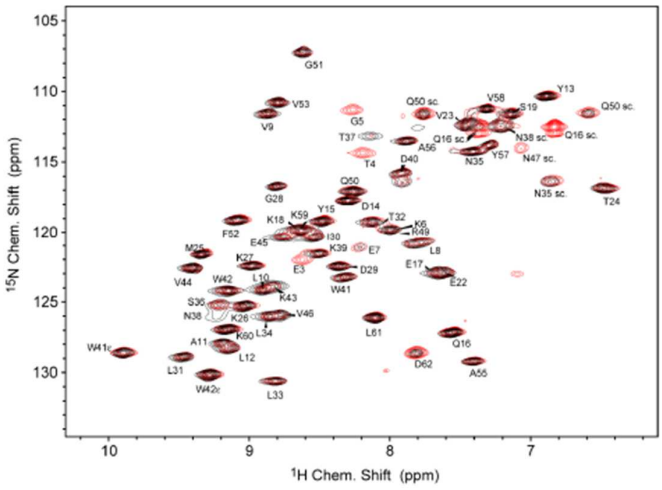

α-spectrin SH3 domain – INEPT or CP transfer – MAS 24 kHz

V. Chevelkov,Y. Xue, R. Linser, N.R. Skrynnikov, B. Reif, *J. Am. Chem. Soc.*, **2010**, 132 (14), pp 5015–5017

NMR: a structural technique?

Structural information
Local probes

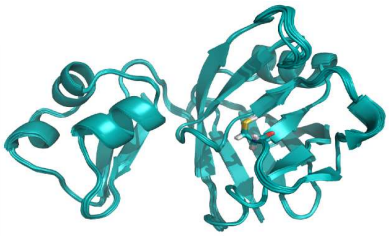

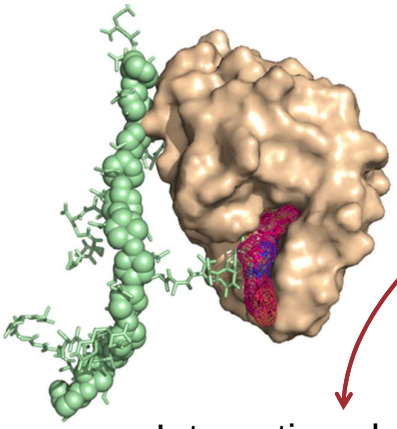

Biomolecular NMR

Dynamical information:
amplitude and
time-scale of motion

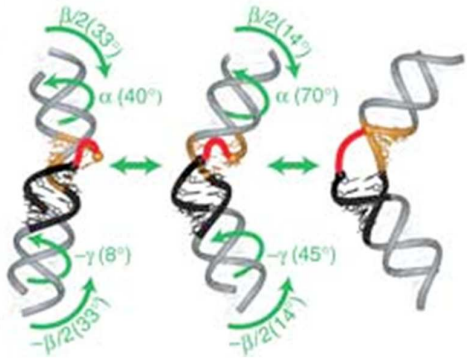

Interactions between
different partner :
interaction site, K_D

Some key parameters and their usage in structural biology

$$H = H_z + H_{cs} + H_{rf} + H_J + H_D + H_Q$$

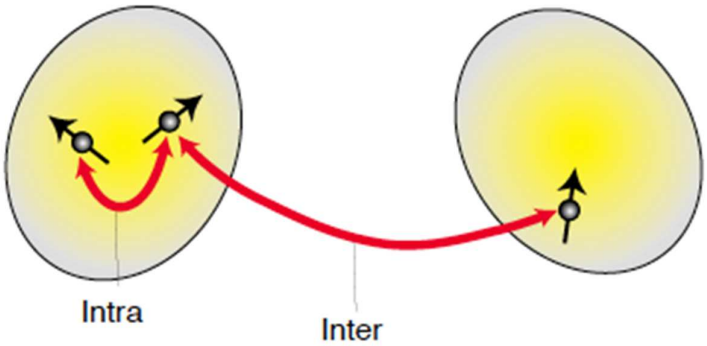

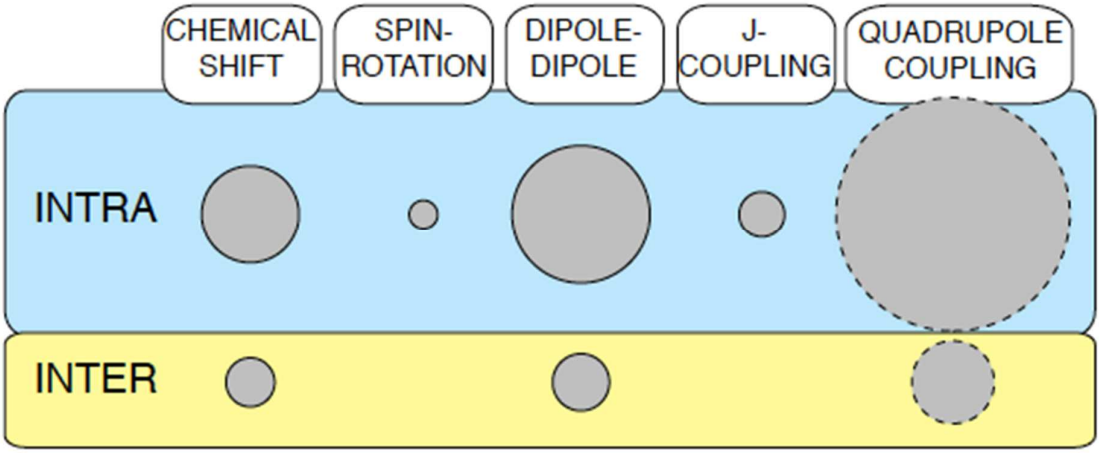

Some key parameters and their usage in structural biology

Chemical shift information

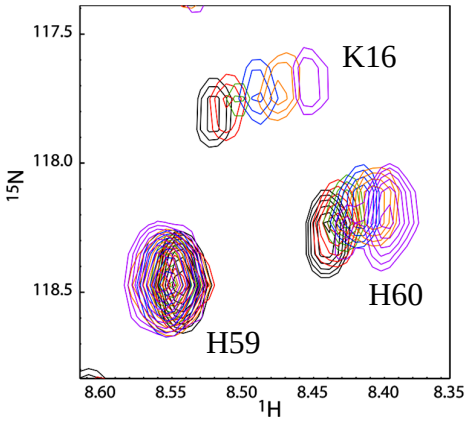

Relaxation

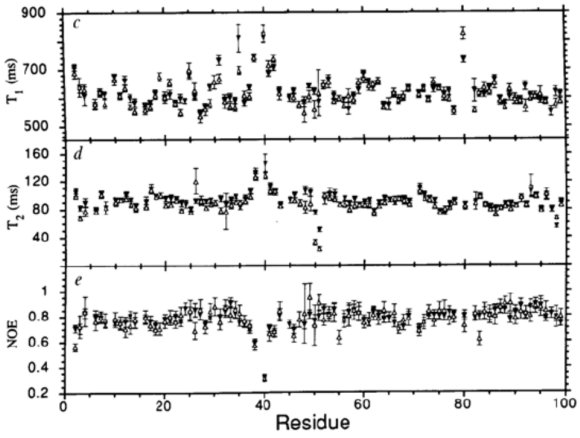

Fig. 1 Inhibitors *a*, DMP323 and *b*, P9941, their respective inhibition constants, K_i, and experimental relaxation parameters *c*, T_1; *d*, T_2; and *e*, NOE values of HIV-1 protease/inhibitor complexes, DMP323 (▼) and P9941 (Δ).

Scalar couplings

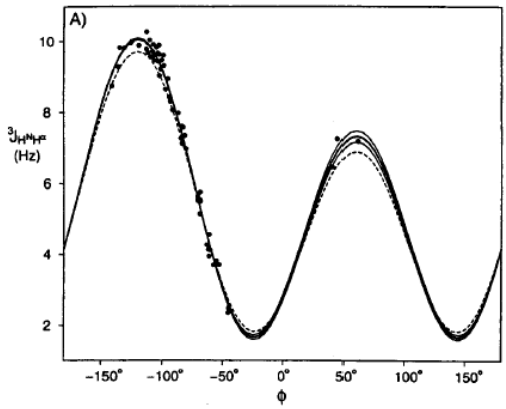

Dipolar interactions

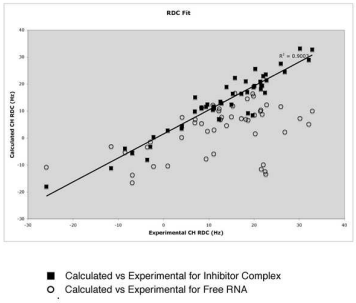

Chemical shift: a finger print of the biomolecule

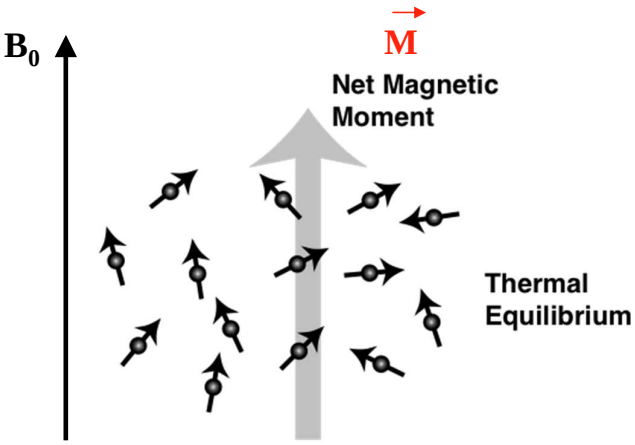

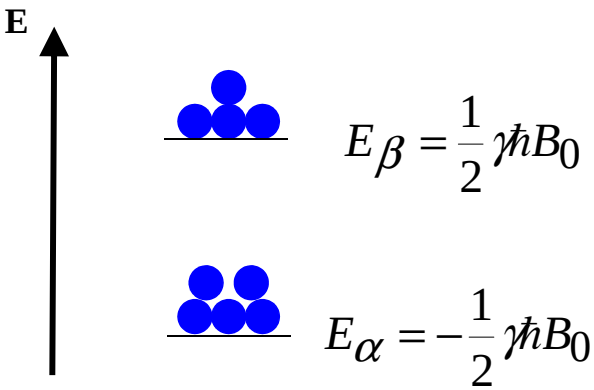

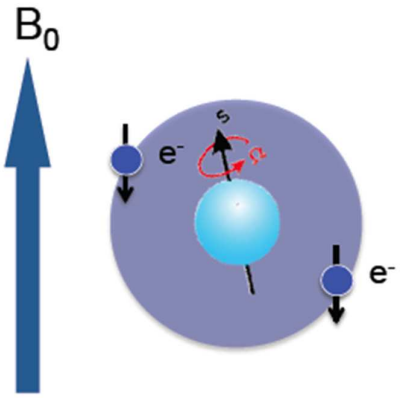

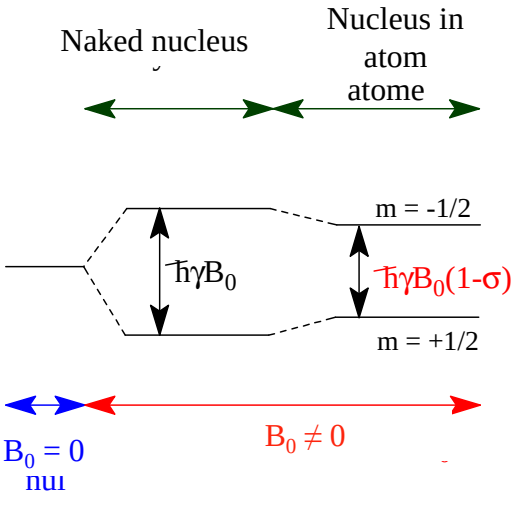

Chemical shift: a finger print of the biomolecule

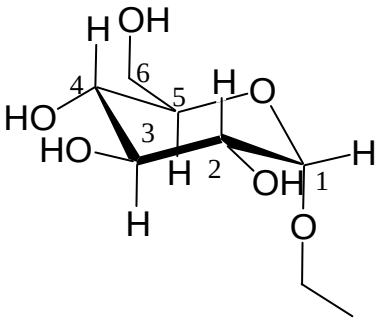

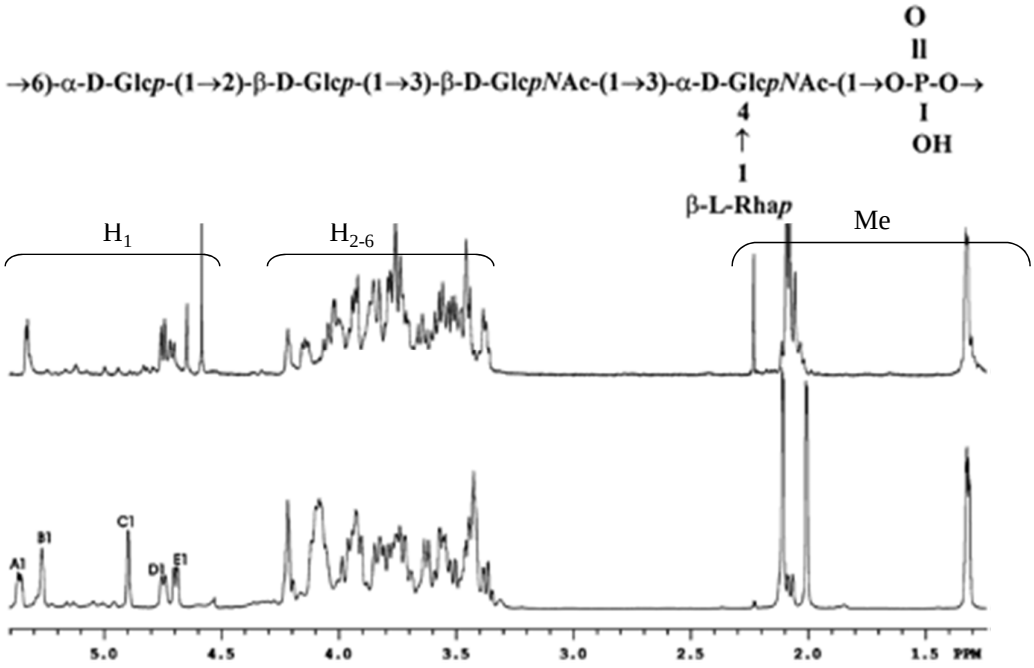

(A) Spectre ^{1}H-NMR (pD 7.8) de O-PS extrait de *C. rodentium*.
(B) Spectre ^{1}H-NMR du derivé de l'oligosaccharide **II** de *C. rodentium* (ATCC 51459)

Eur. J. Biochem. **268**, 5740-5746 (2001)

Chemical shift: a finger print of the biomolecule

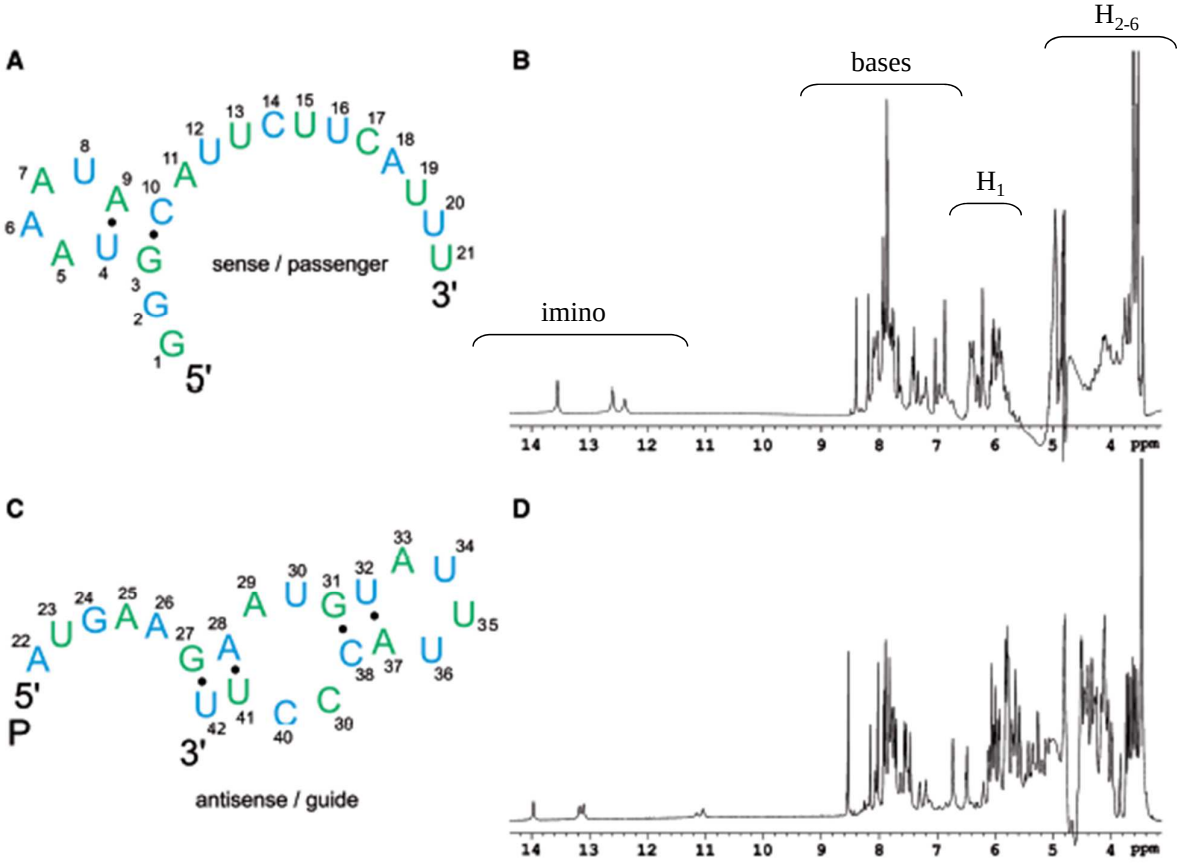

P. Podbevsek, C. R. Allerson, B. Bhat, J Plavec, Nucl. Acids Res., 2010, 7298-7307

Chemical shift: a finger print of the biomolecule

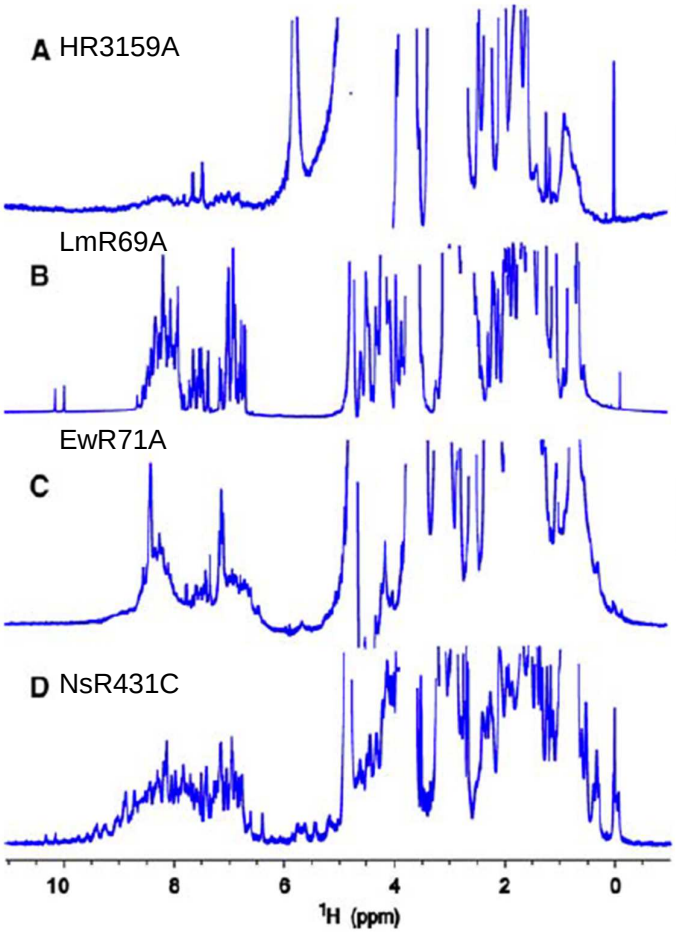

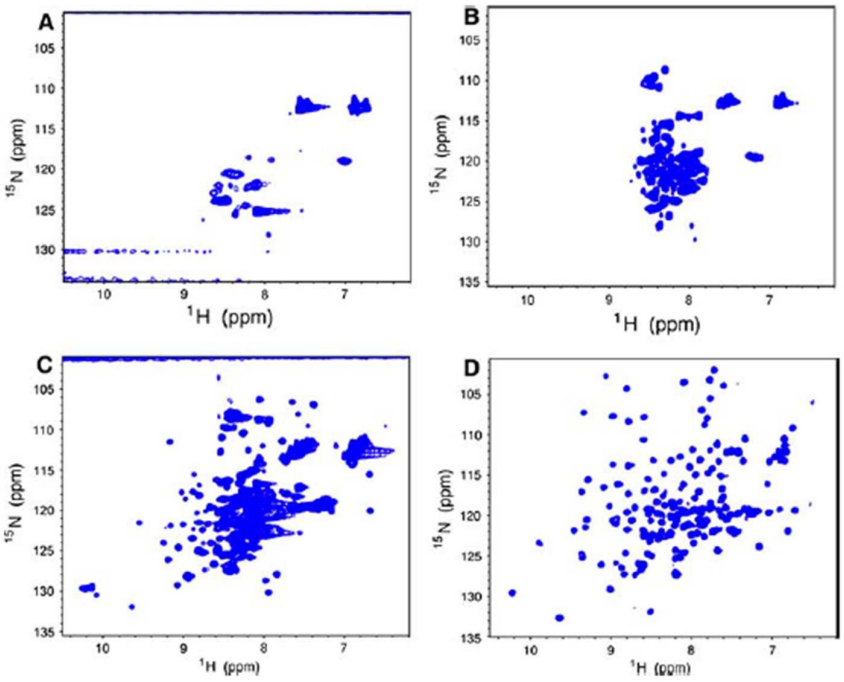

1.7 mm micro-probe at 20 °C
NESG, *J. Biomol NMR* 2010, 46, 11-22

Chemical shift: a structural information content

$$CSI = \delta_{measured} - \delta_{randomcoil}$$

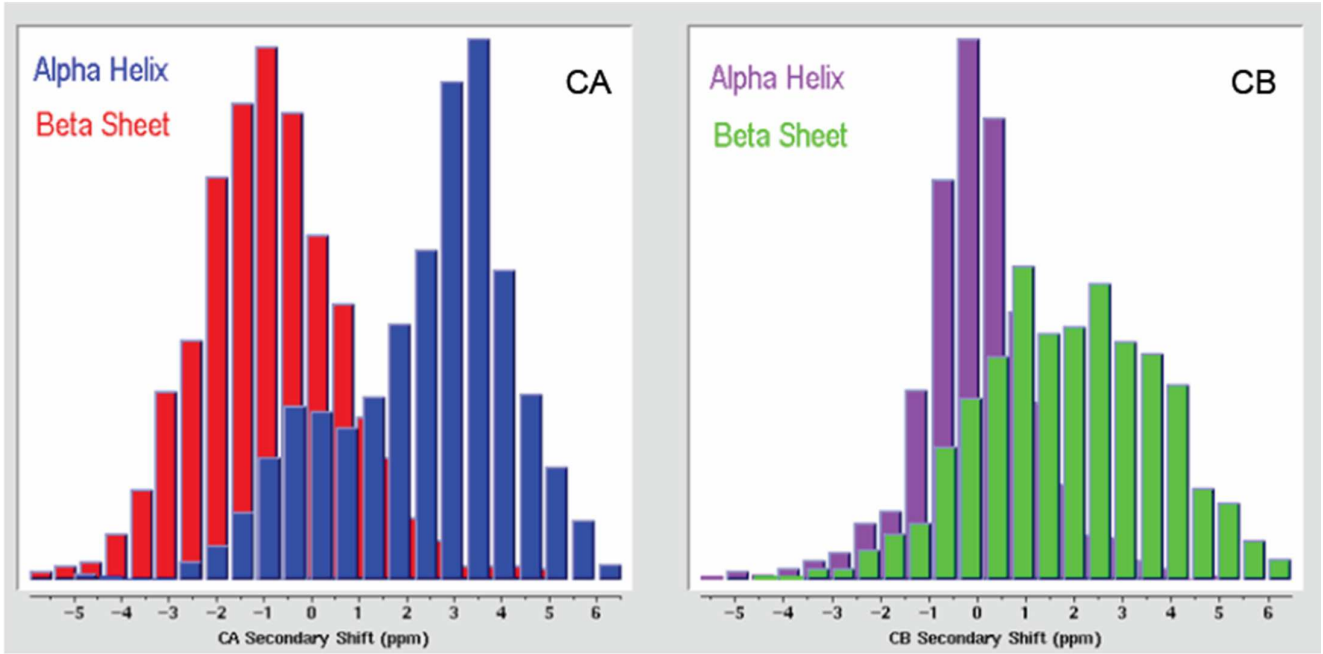

Chemical shift: a structural information content

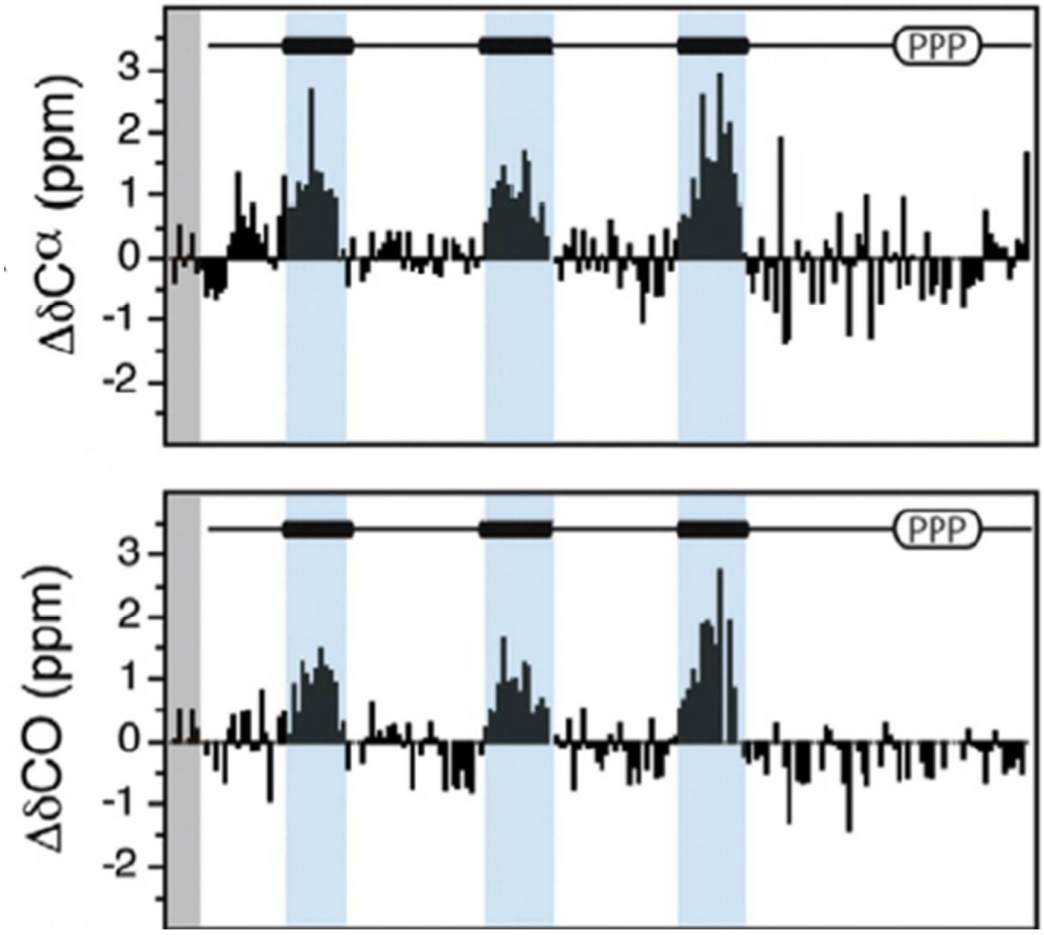

Interest
for IDPs

Chemical shift: a structural information content

Talos+ : http//:spin.niddk.nih.gov/NMRPipe

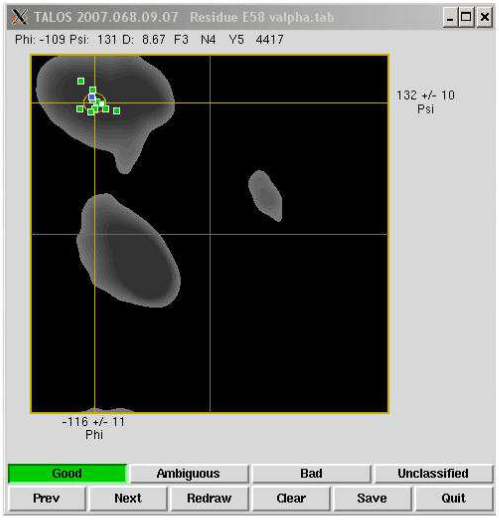

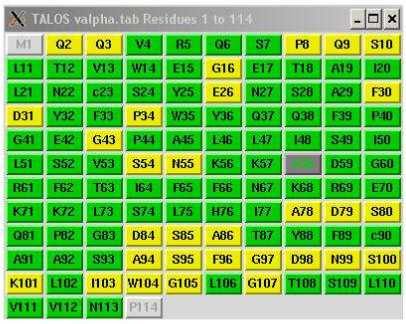

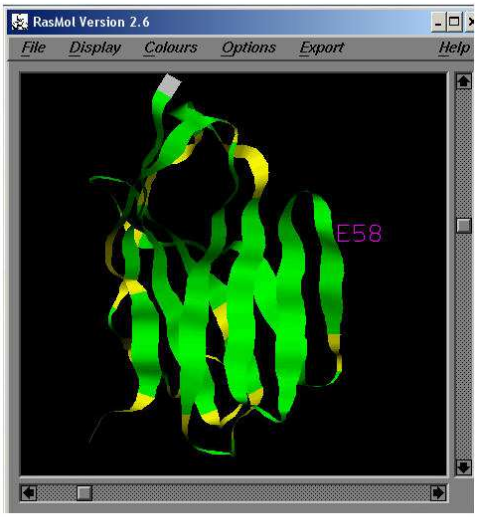

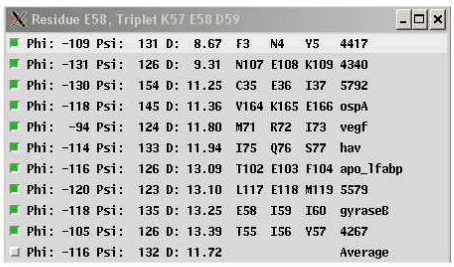

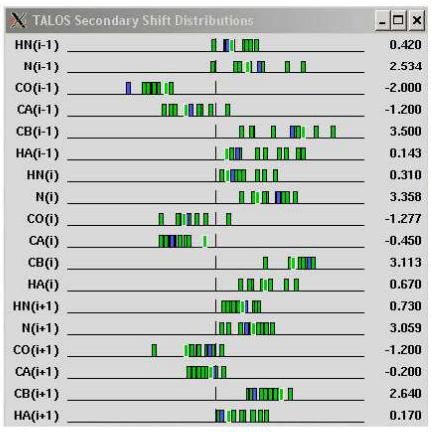

Chemical shift: a structural information content

www.pnas.org/cgi/doi/10.1073/pnas.0800256105 PNAS | March 25, 2008 | vol. 105 | no. 12 | 4685–4690

Consistent blind protein structure generation from NMR chemical shift data

Yang Shen*, Oliver Lange†, Frank Delaglio*, Paolo Rossi‡, James M. Aramini‡, Gaohua Liu‡, Alexander Eletsky§, Yibing Wu§, Kiran K. Singarapu§, Alexander Lemak¶, Alexandr Ignatchenko¶, Cheryl H. Arrowsmith¶, Thomas Szyperski§, Gaetano T. Montelione‡, David Baker†||, and Ad Bax*||

*Laboratory of Chemical Physics, National Institute of Diabetes and Digestive and Kidney Diseases, National Institutes of Health, Bethesda, MD 20892; †Department of Biochemistry and Howard Hughes Medical Institute, University of Washington, Seattle, WA 98195; ‡Center for Advanced Biotechnology and Medicine, Department of Molecular Biology and Biochemistry, and Northeast Structural Genomics Consortium, Rutgers, The State University of New Jersey, and Robert Wood Johnson Medical School, Piscataway, NJ 08854; §Departments of Chemistry and Structural Biology and Northeast Structural Genomics Consortium, University at Buffalo, State University of New York, Buffalo, NY 14260; and ¶Ontario Cancer Institute, Department of Medical Biophysics, and Northeast Structural Genomics Consortium, University of Toronto, Toronto, ON, Canada M5G 1L5

Protein NMR chemical shifts are highly sensitive to local structure. A robust protocol is described that exploits this relation for *de novo* protein structure generation, using as input experimental parameters the $^{13}C^{\alpha}$, $^{13}C^{\beta}$, $^{13}C'$, ^{15}N, $^{1}H^{\alpha}$ and $^{1}H^{N}$ NMR chemical shifts. These shifts are generally available at the early stage of the traditional NMR structure determination process, before the collection and analysis of structural restraints. The chemical shift based structure determination protocol uses an empirically optimized procedure to select protein fragments from the Protein Data Bank, in conjunction with the standard ROSETTA Monte Carlo assembly and relaxation methods. Evaluation of 16 proteins, varying in size from 56 to 129 residues, yielded full-atom models that have 0.7–1.8 Å root mean square deviations for the backbone atoms relative to the experimentally determined x-ray or NMR structures. The strategy also has been successfully applied in a blind manner to nine protein targets with molecular masses up to 15.4 kDa, whose conventional NMR structure determination was conducted in parallel by the Northeast Structural Genomics Consortium. This protocol potentially provides a new direction for high-throughput NMR structure determination.

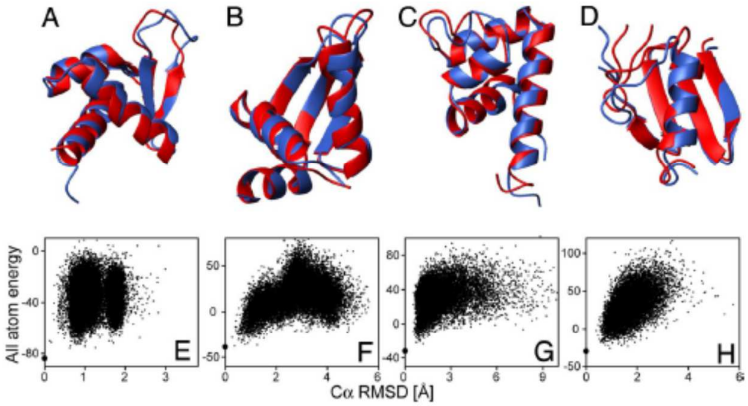

Fig. 4. Results from blind CS-ROSETTA structure generation for four structural genomics targets (Table 2). The remaining five are in SI Fig. 12. (*A–D*) Superposition of lowest-energy CS-ROSETTA models (red) with experimental NMR structures (blue), with superposition optimized for ordered residues, as defined in the footnote to SI Table 5. (*E–H*) Plots of rescored (Eq. 1) ROSETTA all-atom energy versus C^{α} rmsd relative to the lowest-energy model (bold dot on vertical axis). (*A* and *E*) StR82. (*B* and *F*) RpT7. (*C* and *G*) VfR117. (*D* and *H*) NeT4.

Chemical shift: a tool for interactions

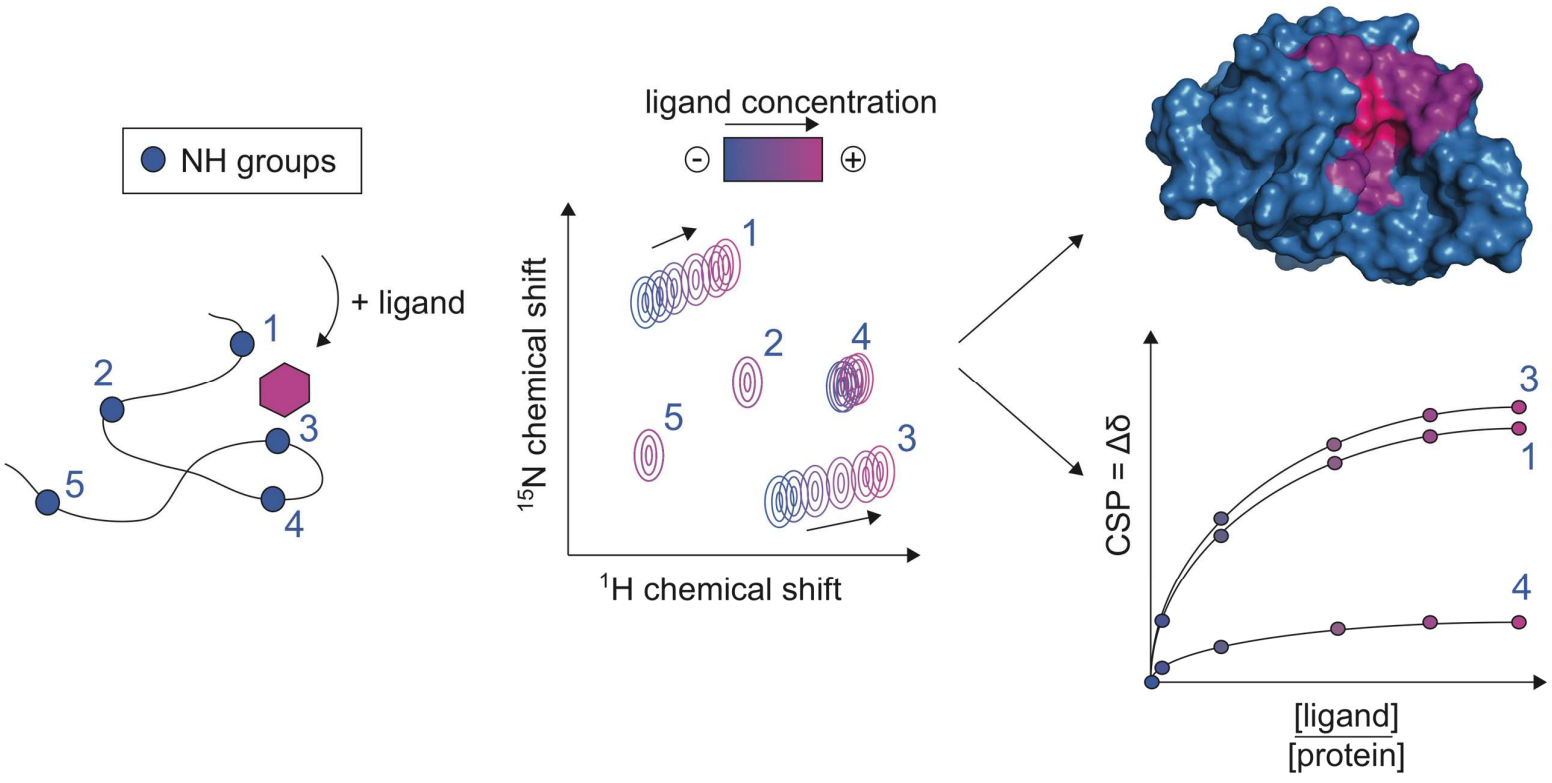

Chemical shift and chemical exchange (µs-ms)

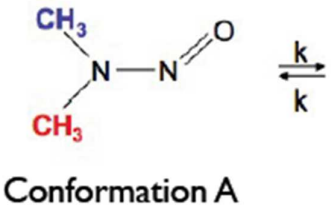

k
k

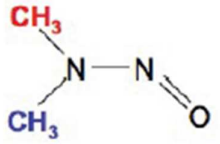

Conformation A Conformation B

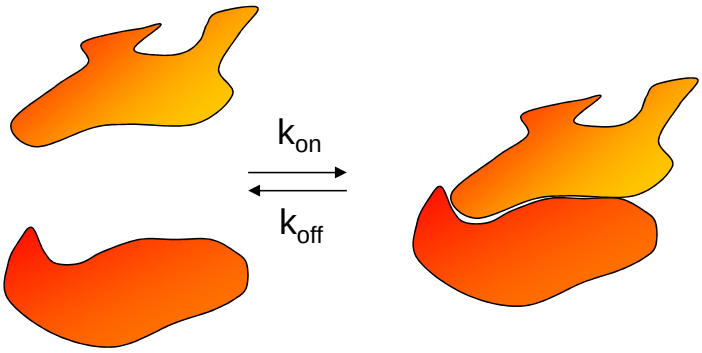

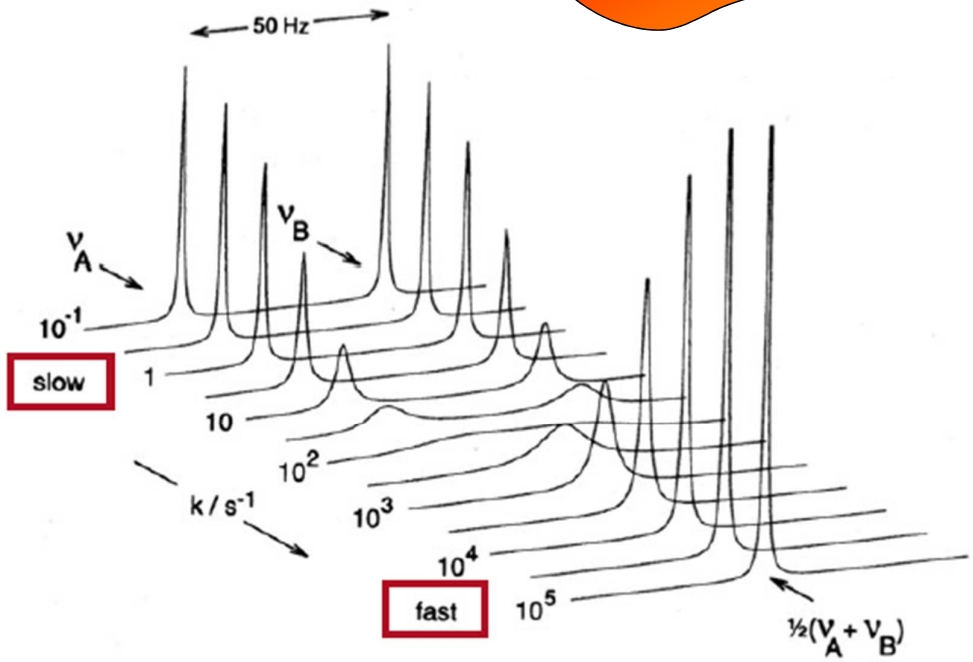

Chemical shift: a tool for interactions

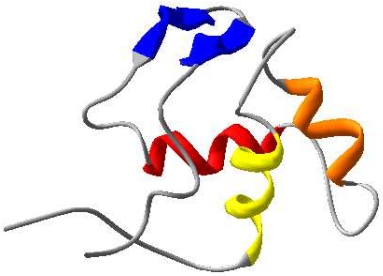

+

→ **Complex?**

[^{13}C,^{15}N]-BlaI-NTD 0.1 mM DNA(12 bp) 0-0.45 mM

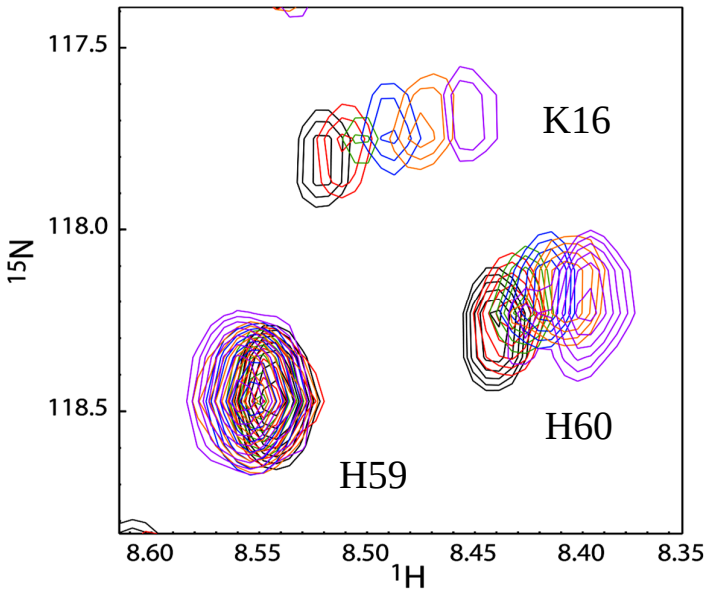

BlaI	DNA
1	0
1	0.3
1	0.7
1	1.5
1	2.5
1	4.5

Chemical shift: a tool for interactions

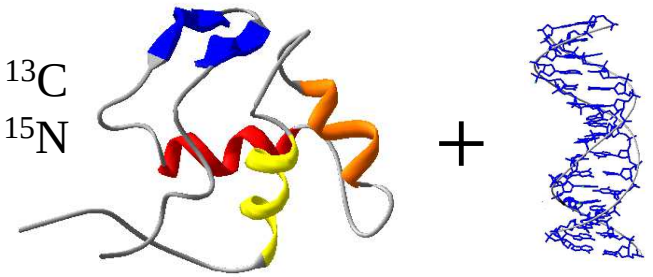

Complexe

20 ^{1}H protein resonances with significant chemical shifts

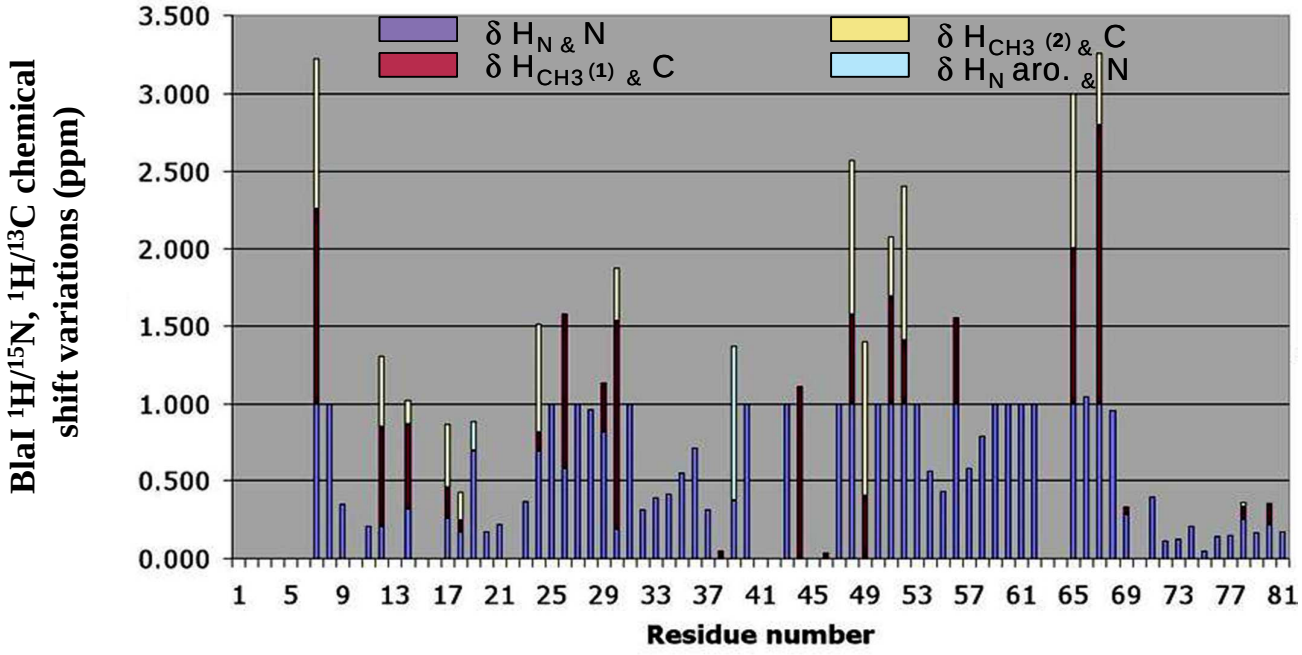

Chemical shift: a tool for interactions

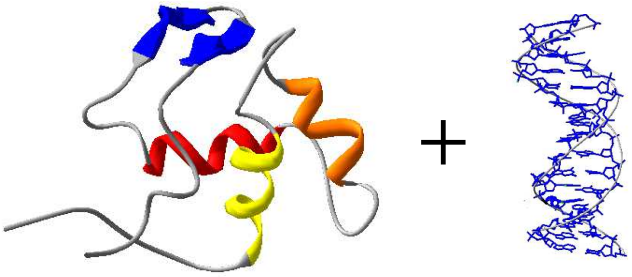

BlaI-NTD DNA

Complex

Kd ~ 100-300 µM

Titration de BlaI par ADN

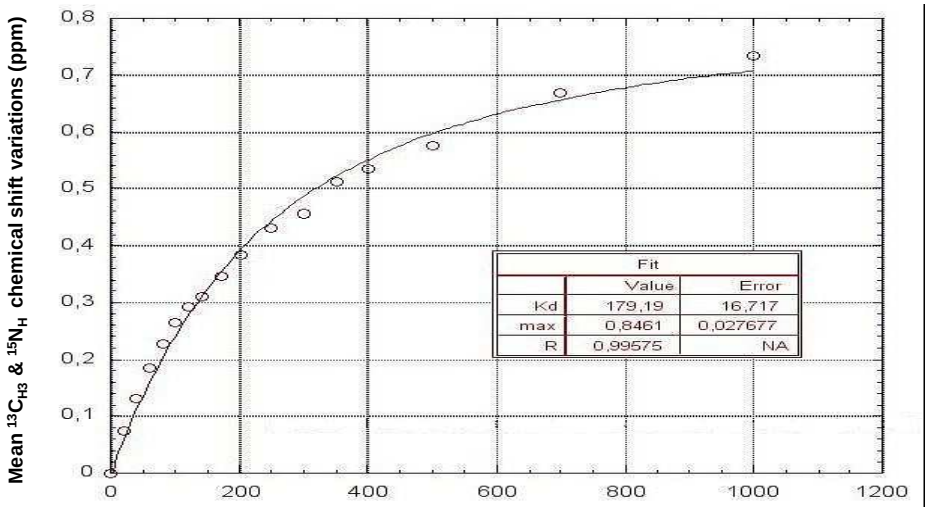

Chemical shift: a tool for interactions

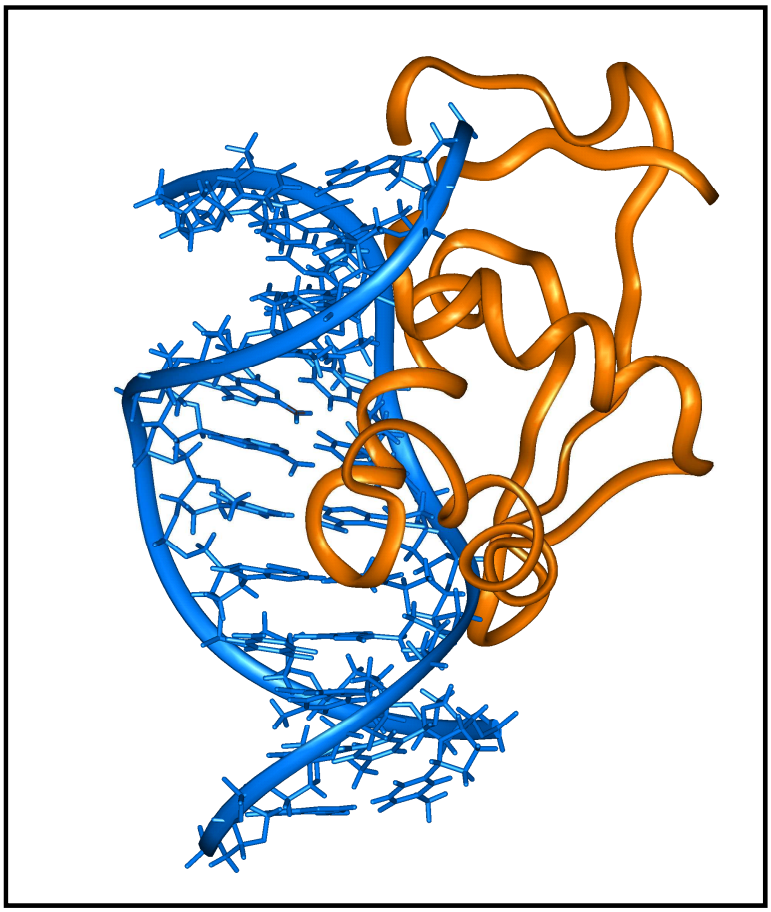

Relaxation

E

RF pulse

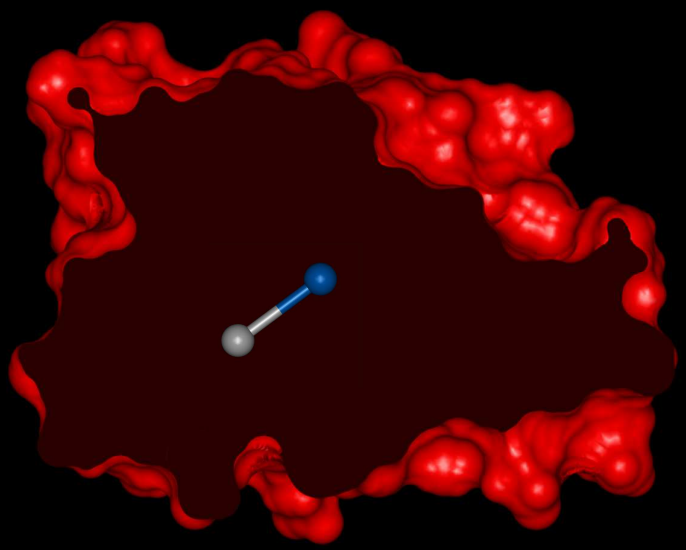

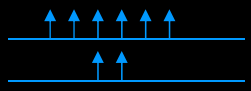

1 transition every 3.10^{13} years

Excitation of spin-state

$W_0 = \mu_0\mu^2/(2h\lambda^3) = 10^{-21}\ s^{-1}$ (^{1}H @ 11.7 T)

Spontaneous emission is negligible at NMR frequencies!

($W_0 = 10^8\ s^{-1}$ for electronic transitions at optical frequencies)

Relaxation

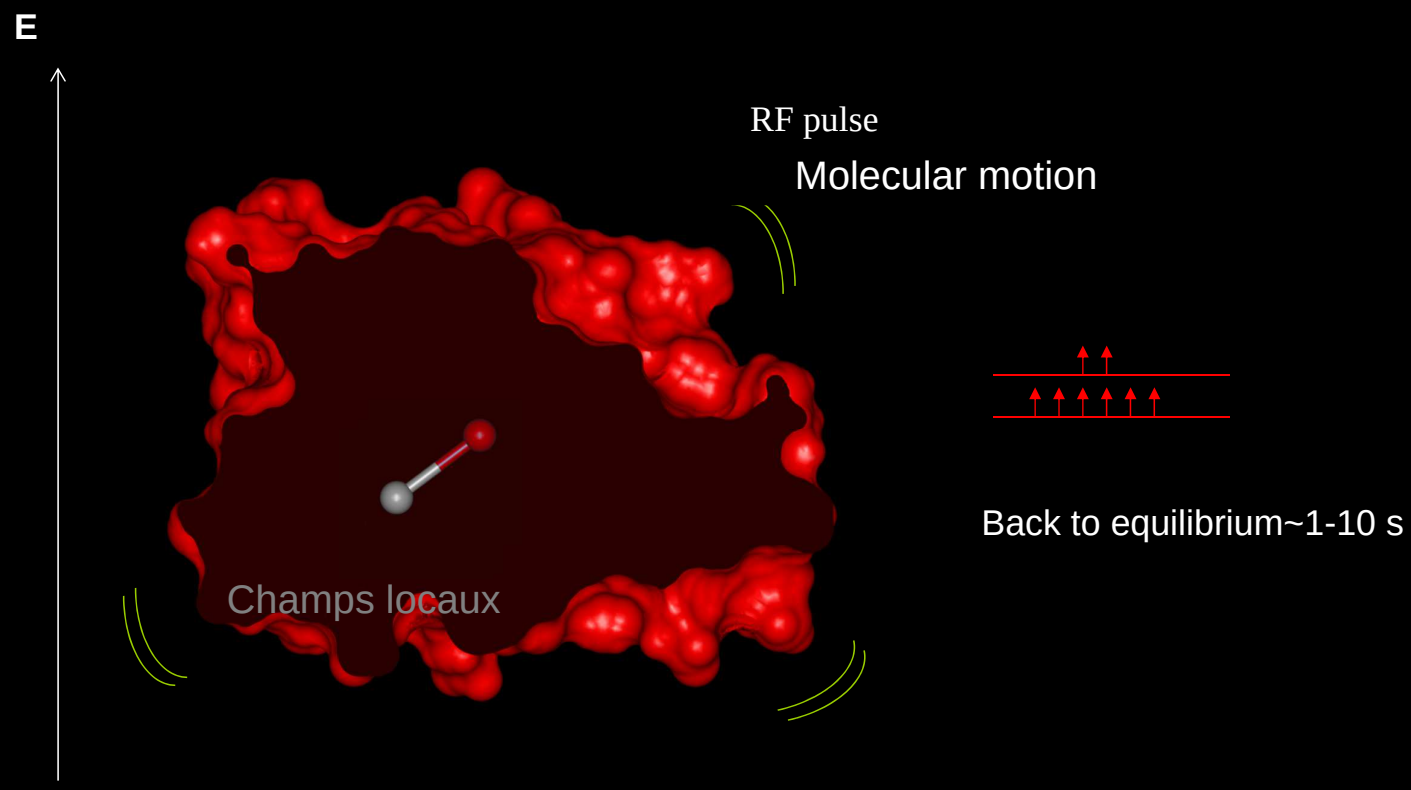

Relaxation de l'état de spin

Relaxation: an interaction tool

Interaction Monastrol/EG5

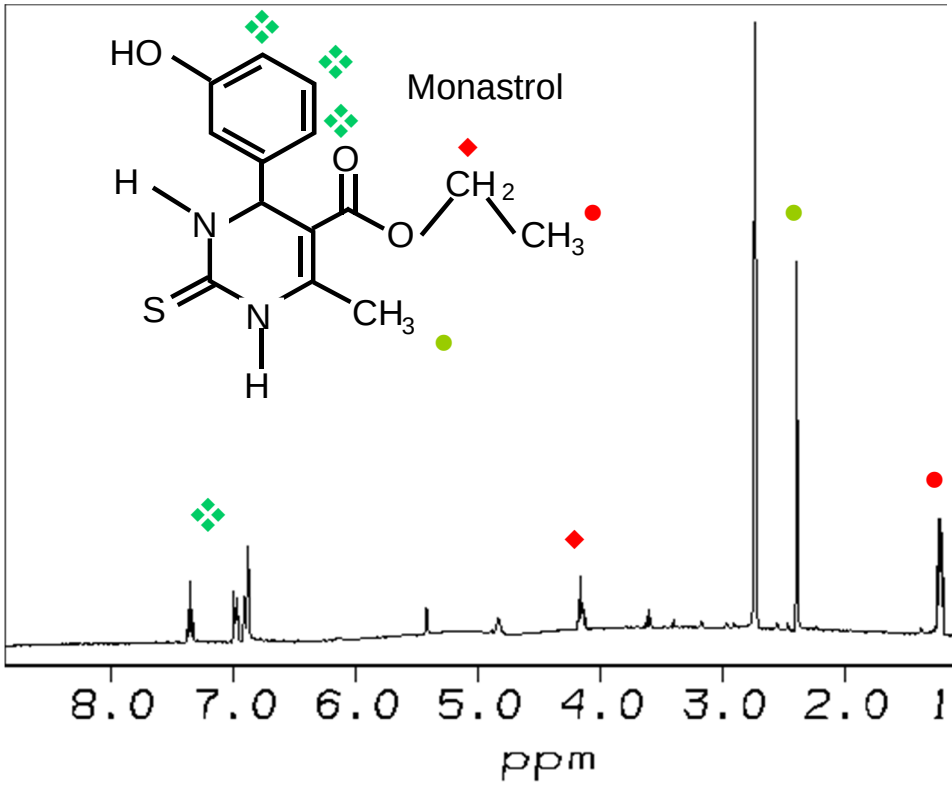

Microtubule-dependent kinesin-like protein Eg5

Relaxation: an interaction tool

$[EG5_{(2\text{-}386)}] = [Monastrol] = 40\ \mu M$

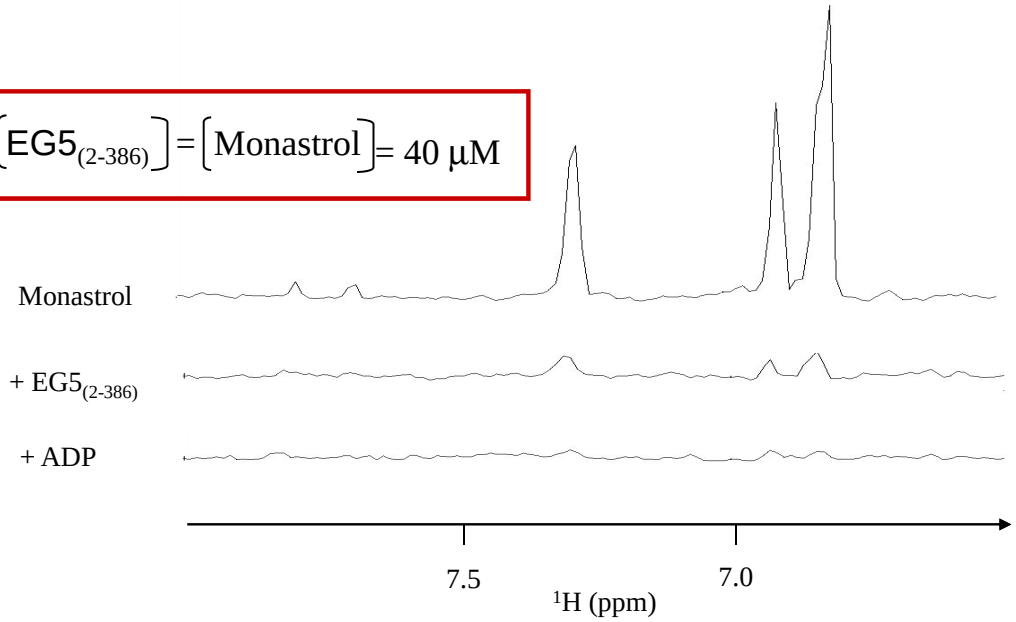

	free monastrol	K_d
Monastrol	100 %	
+ $EG5_{(2\text{-}386)}$	20 %	~ 5 µM
+ ADP	< 5%	> 0.4 µM

$$K_d = \frac{P_{free} \bullet M_{free}}{PM} = \frac{F_{free}^{\ 2}}{1 - F_{free}} \bullet M_0$$

Relaxation: a dynamical information

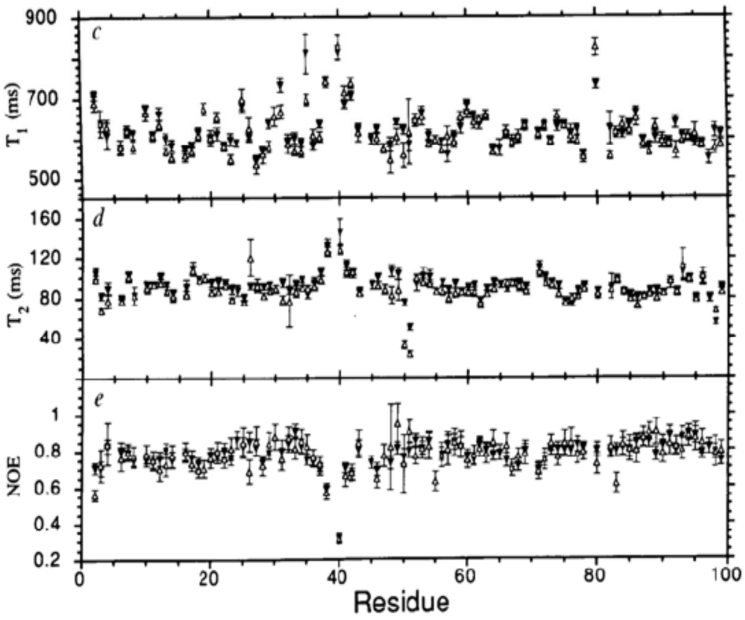

Fig. 1 Inhibitors *a*, DMP323 and *b*, P9941, their respective inhibition constants, K_i and experimental relaxation parameters *c*, T_1; *d*, T_2; and *e*, NOE values of HIV-1 protease/inhibitor complexes, DMP323 (▼) and P9941 (Δ).

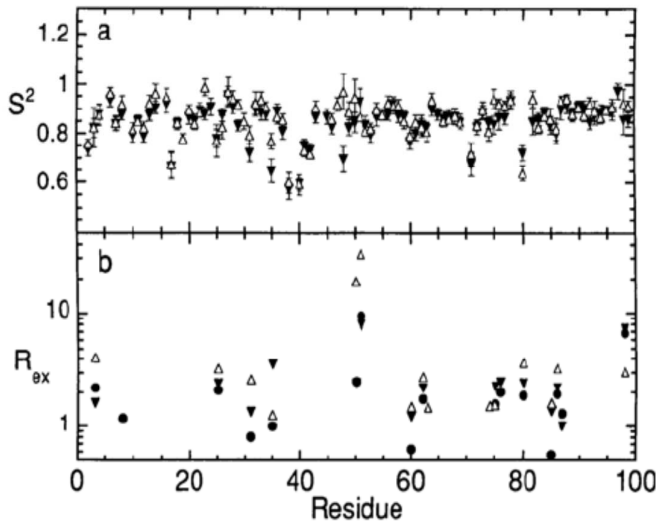

Fig. 2 *a*, Generalized order parameters (S^2) and *b*, the chemical exchange contribution to $1/T_2$ (R_{ex}), plotted as a function of residue number for the two complexes (▼) DMP323 using three relaxation parameters, T_1, T_2 at 500 MHz and NOE at 600 MHz; (●) DMP323 using four relaxation parameters, T_1, T_2 at 500 MHz a
parameters, T_1, T_2 at 500 MHz ar

a Mobility : 1 - 100 ps

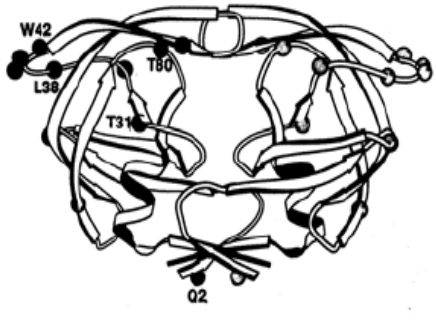

[1] L. Nicholson, T. Yamazaki, D.A. Torchia, S. Grzesiek, A. Bax, S.J. Stahl, J.D. Kaufman, P.T. Wingfield, P.Y.S. Lam, P.K. Jadhav, C.N. Hodge, P.J. Domaille, and C.-H. Chang: Flexibility and function in HIV-1 protease. Nature Structural Biology 2, 274-279, 1995.

Scalar couplings

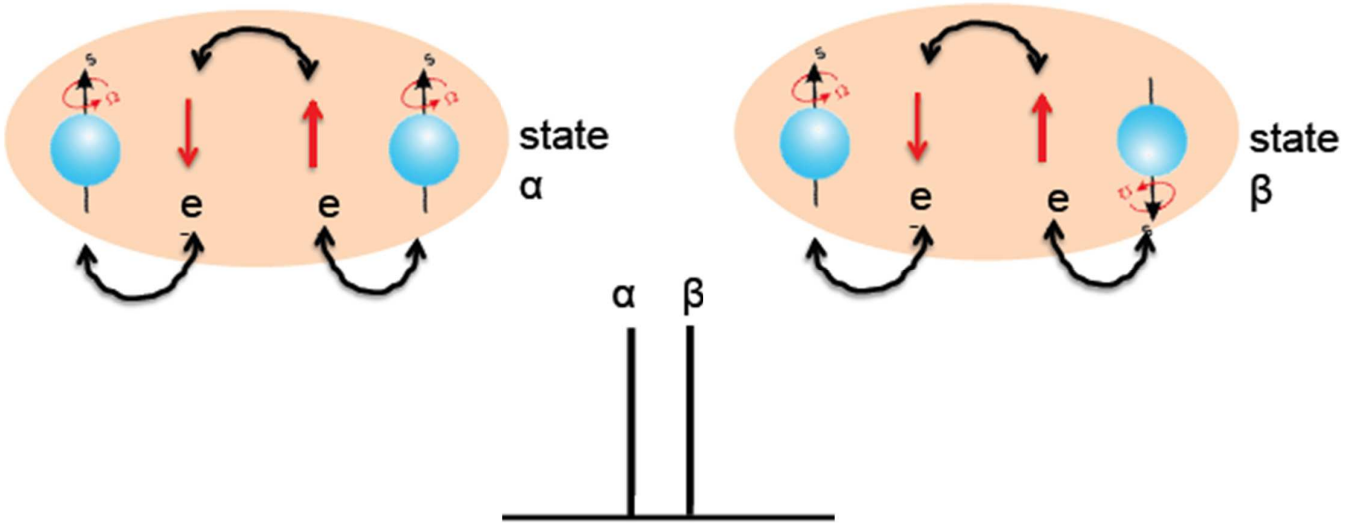

^{1}H-NMR spectrum of $C_6H_{12}O$

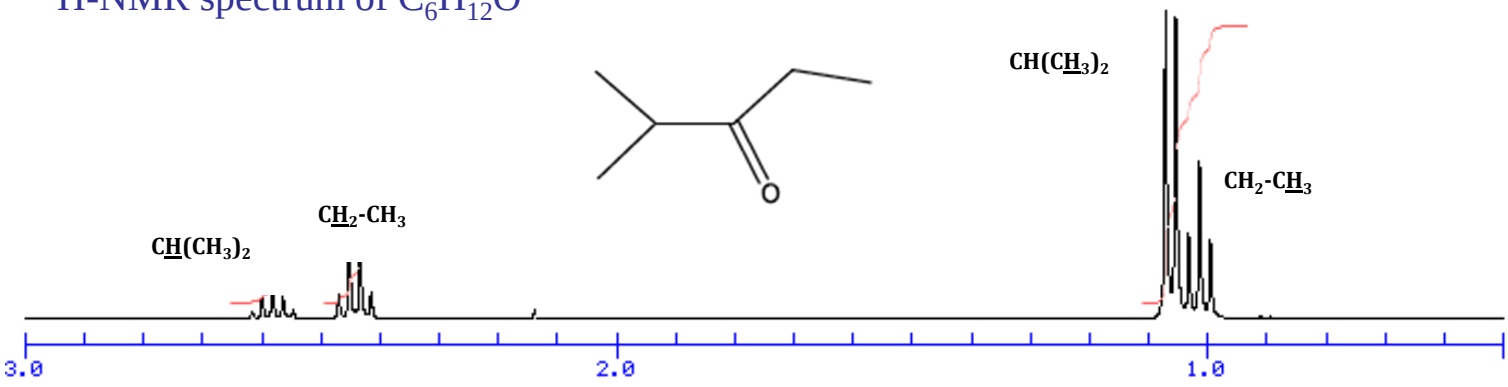

Scalar couplings: a structural information content

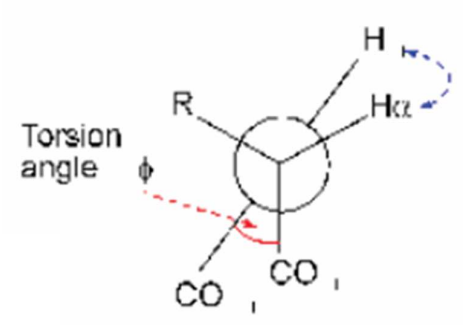

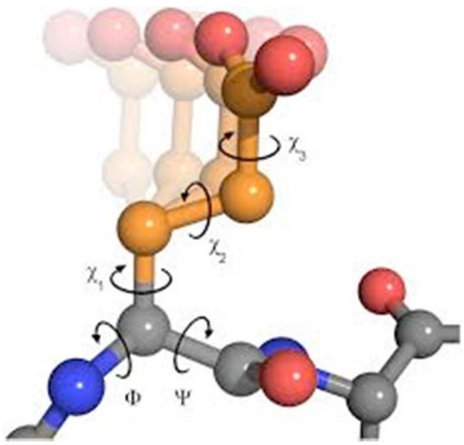

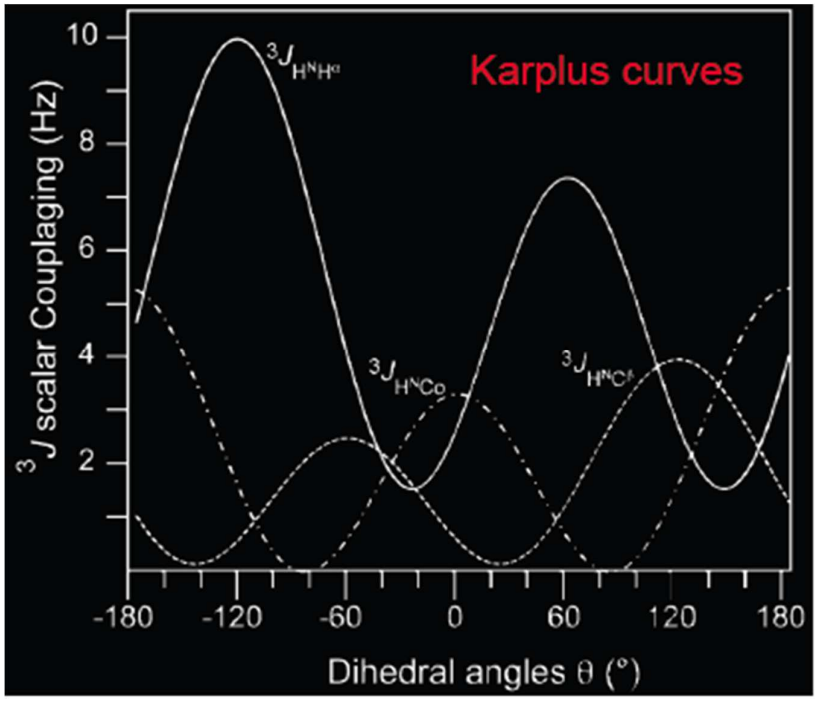

$^3J_{Ha\text{-}Hb} = 6.98\cos^2(\phi\text{-}60) - 1.38\cos(\phi\text{-}60) + 1.72$

J. Wang, A.Bax, J. Am. Chem. Soc., **1996**, 118, 2492

Scalar couplings: a structural information content

Oligosaccharide sugar-pucker

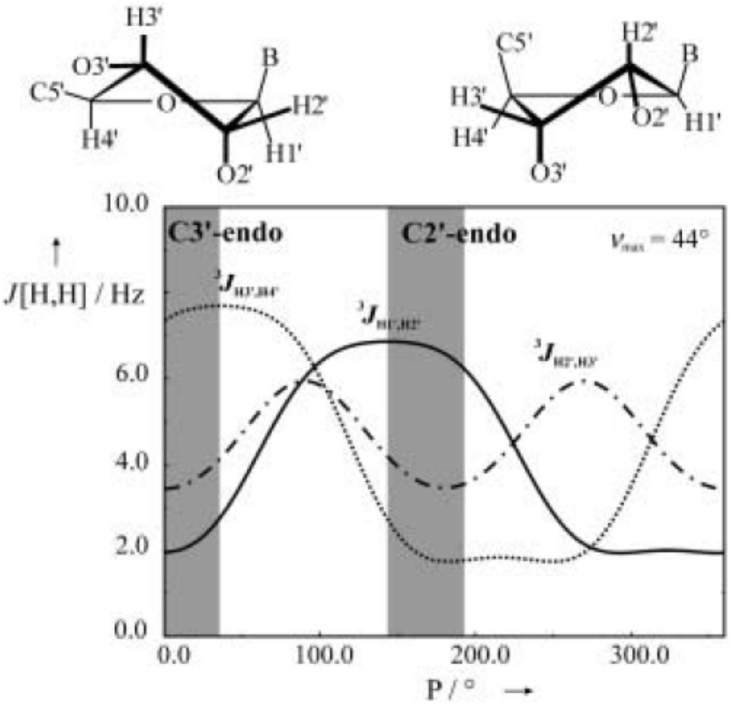

NMR Spectroscopy of RNA
B. Furtig, C. Richter, J. Wohnert and H. Schwalbe
ChemBioChem, **2003**, 4, 936 - 962

Figure 27. *Karplus relation of ^{3}J(H1′,H2′), ^{3}J(H2′,H3′), and ^{3}J(H3′,H4′) coupling constants depending on the pseudorotation phase P at a pseudorotation amplitude ν_{max} of 44°.*

Scalar couplings: a structural information content

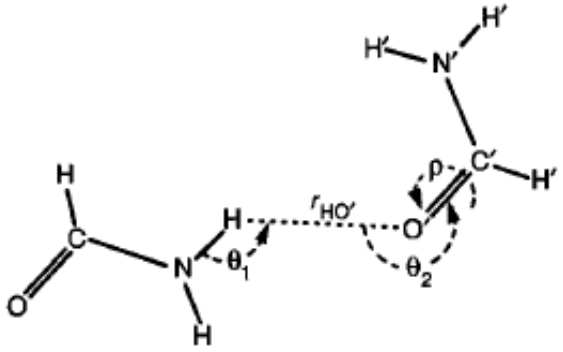

Cordier, Grzesiek, *J. Am. Chem. Soc.*, **1999**, 1601-1602

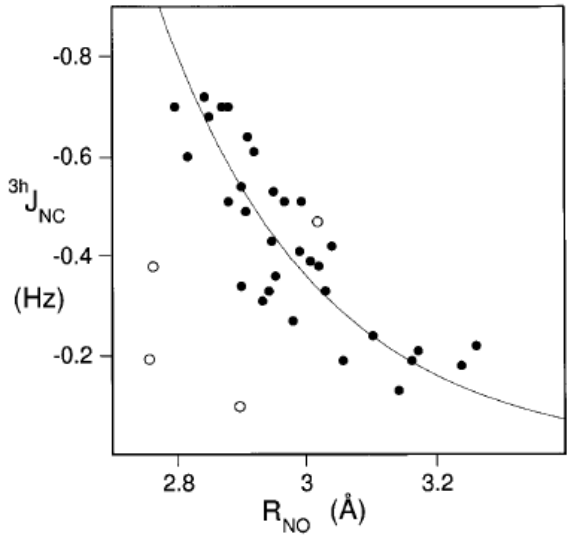

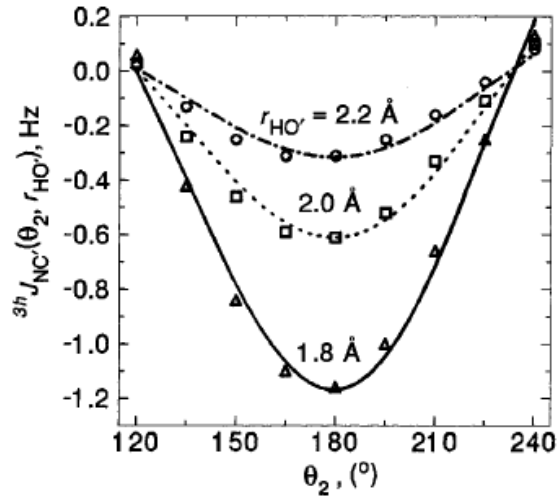

$$r_{NO} = 2.75 - 0.25\ln(-{}^{3h}J_{NC'}) \pm 0.06\text{Å}$$

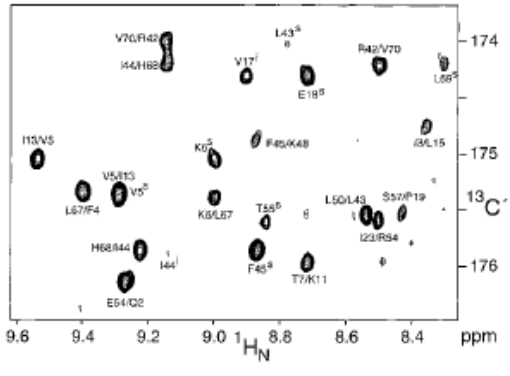

Dipolar interactions

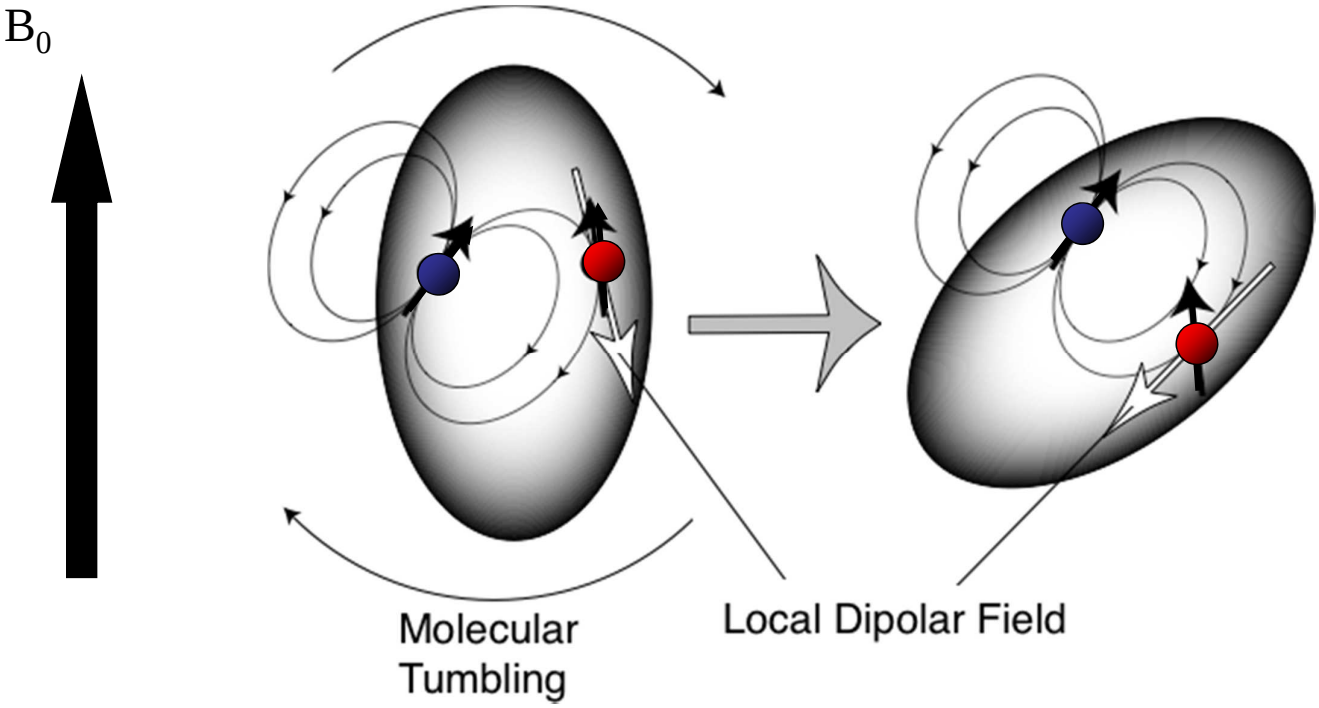

Dipolar interactions

Spin-pairs in different orientations have different dipolar couplings

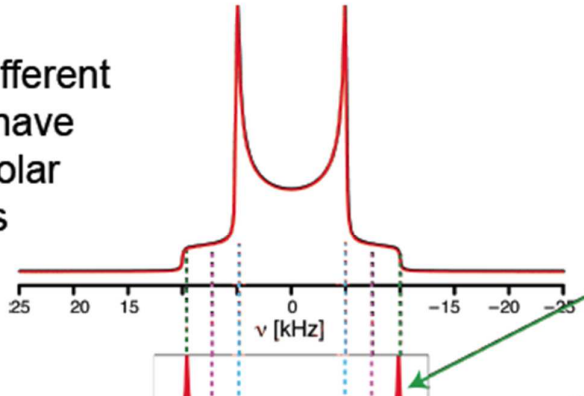

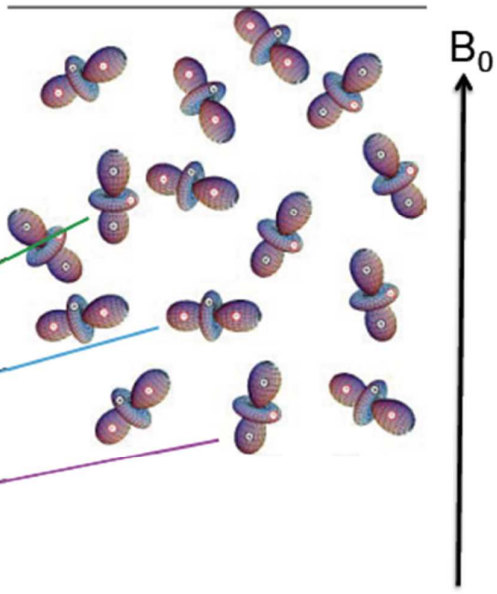

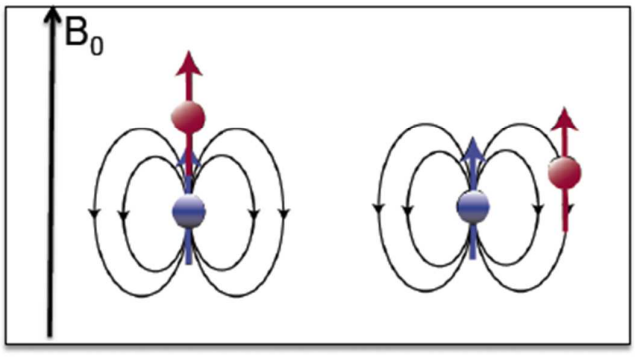

BUT: the fast rotation of molecules in solution averages the dipolar coupling to ZERO

Dipolar interactions: a structural information content

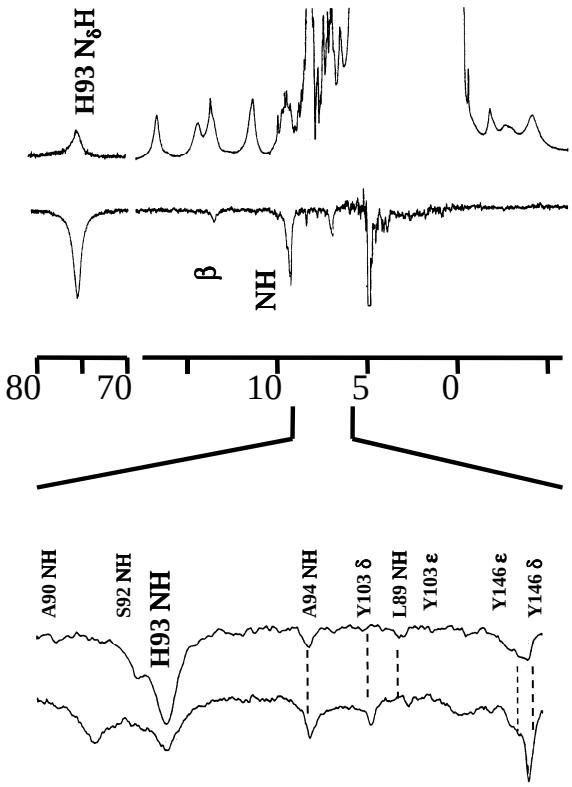

^{1}H NOE-difference spectrum of sperm whale myoglobin

Overhauser effect

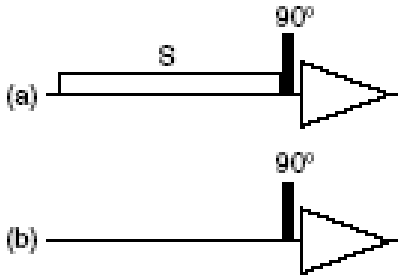

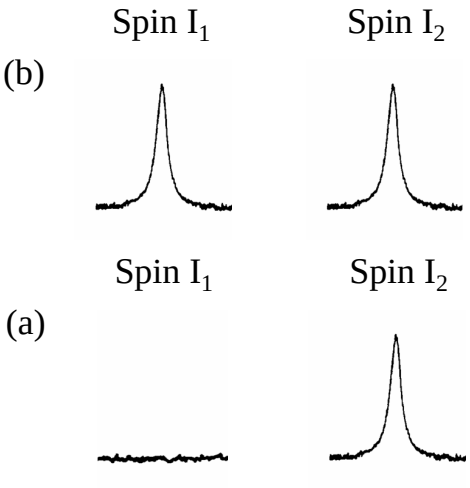

Dipolar interactions: a structural information content

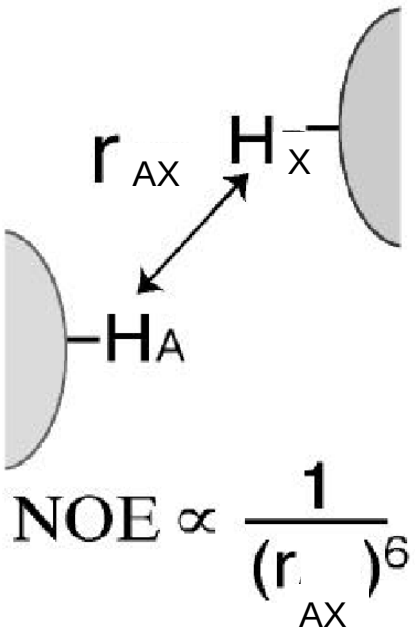

Overhauser effect

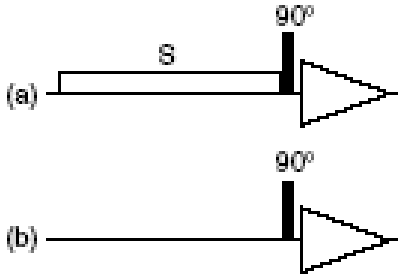

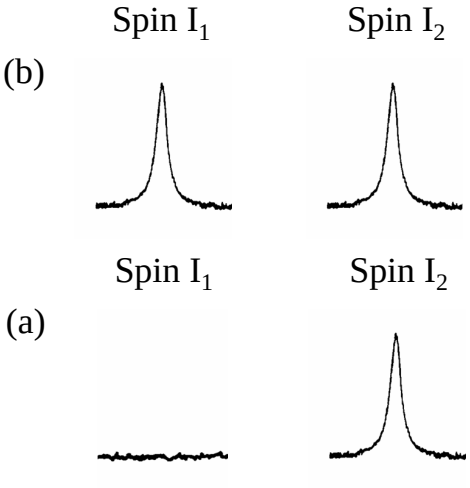

Dipolar interactions: a structural information content

RNA

Overhauser effect

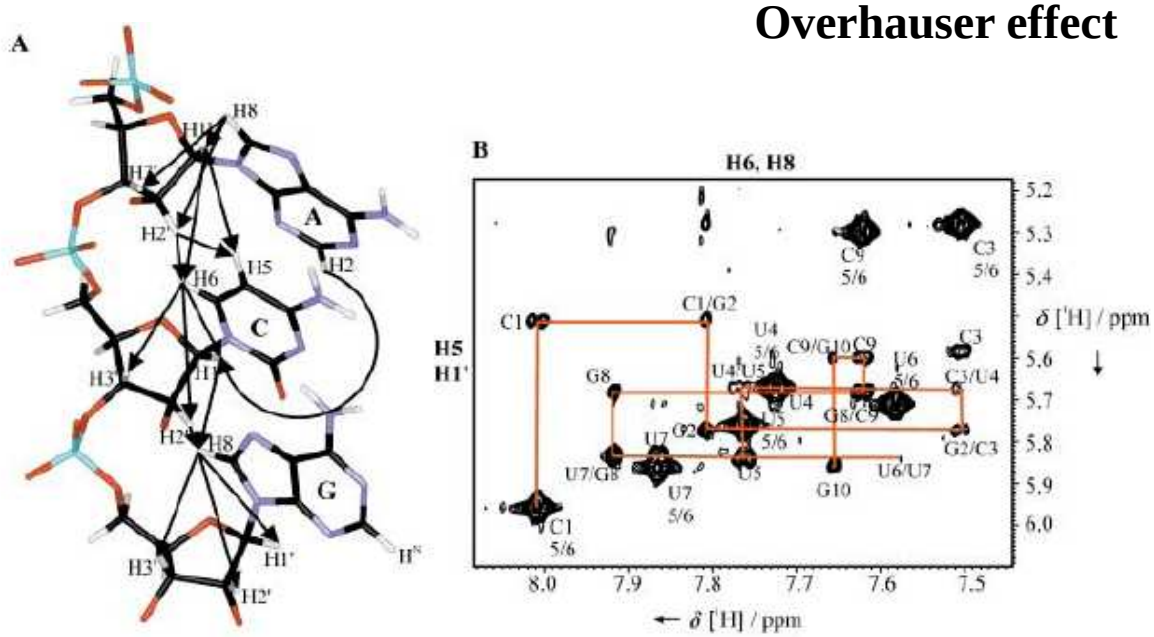

Figure 17. A) Schematic representation of the sequential assignment strategy in helical A-form RNA for nonexchangeable protons. The arrows show the intraresidual NOE connectivities between the aromatic and the sugar protons H1' – H3' and the sequential NOE correlation between the H3' – H6, H8 protons and the H5 – H1' protons. The sequential assignment of the helical A-form conformation is possible by determination of these NOE cross-peaks. In addition to the exchangeable protons, only the intercatenar NOE interactions between the adenine H2 and H1' of the corresponding RNA strand give information about the helical conformation. B) An example for the NOESY assignment procedure shown for the cUUUUg loop RNA. The NOESY spectrum was recorded in D_2O at 600 MHz and the mixing time was 300 ms. Annotation by using two residues indicates connectivities due to sequential NOE contacts and annotation with one nucleotide indicates intraresidual NOE interactions.

B. Furtig, C. Richter, J. Wohnert and H. Schwalbe
ChemBioChem, **2003**, 4, 936 - 962

Dipolar interactions: a structural information content

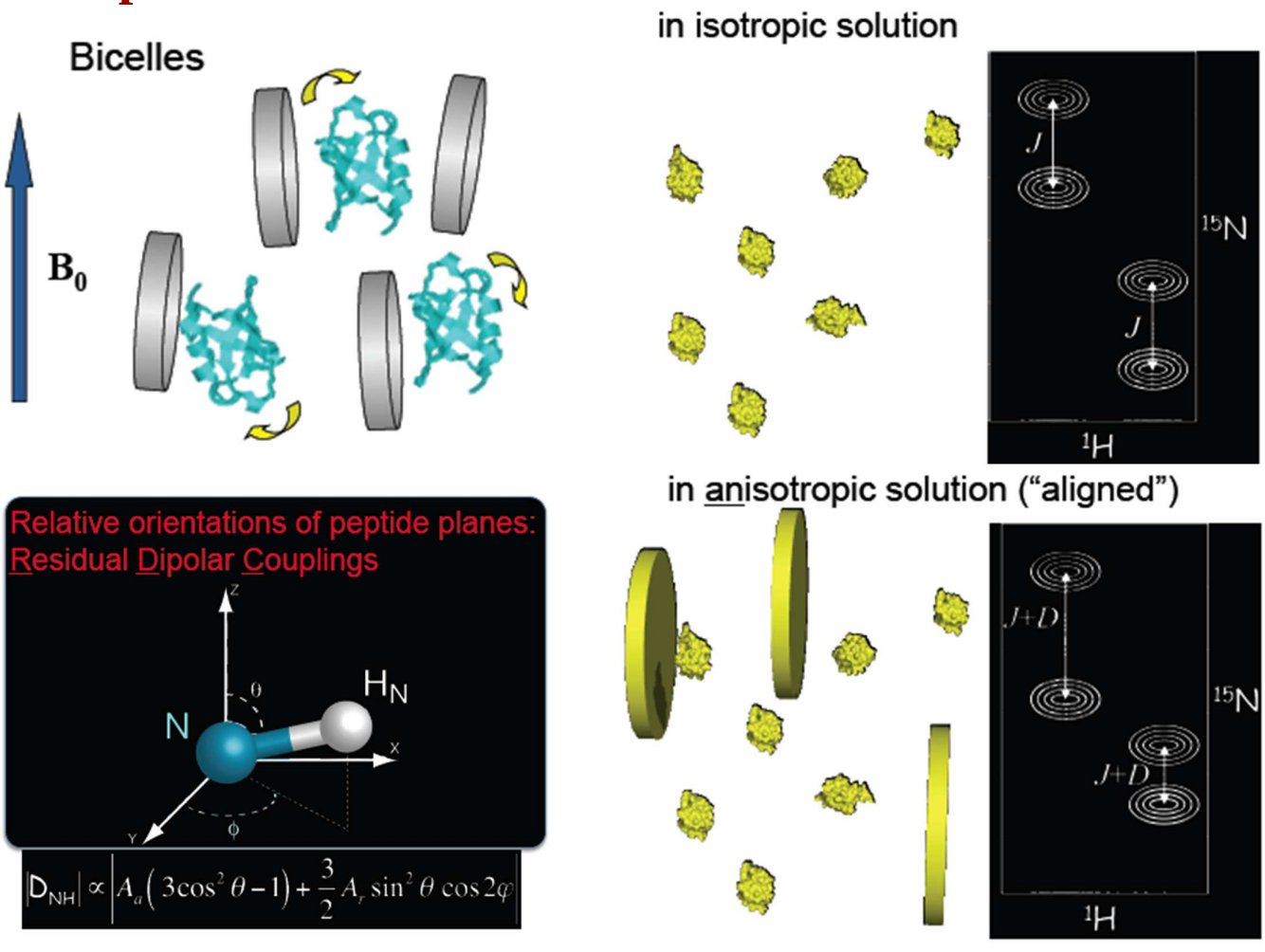

Dipolar interactions: a structural information content

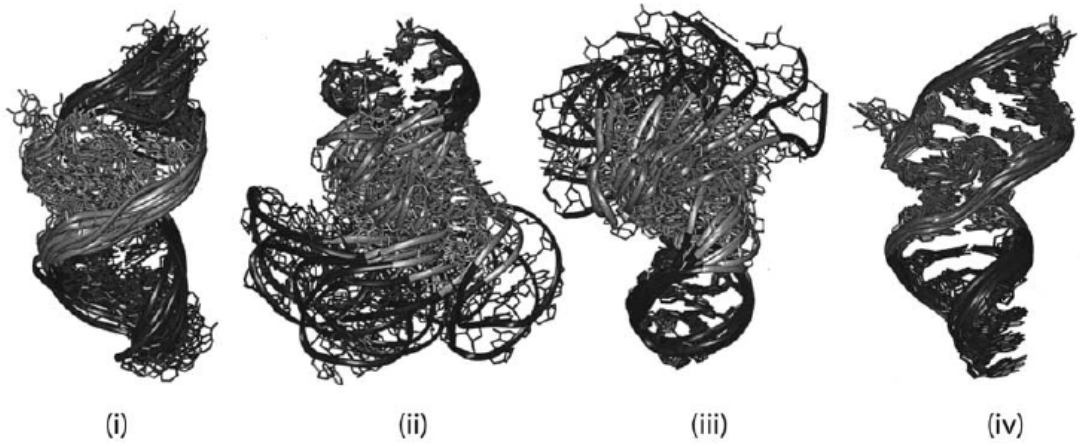

Calculation of the structure of the theophylline-binding RNA aptamer using ^{13}C–^{1}H residual dipolar couplings and restrained molecular dynamics.
The panels (i–iii) represent the lowest target-function conformations from the nOe/J-coupling ensemble: (i) superposed using all the nucleic acids; (ii) superposed using the 30–50 stem I region; and (iii) superposed using the stem II—loop region. (iv) The structural ensemble represents the nOe/J-coupling/RDC ensemble superposed on all nucleic acids.

Dipolar interactions: an intermolecular interaction tool

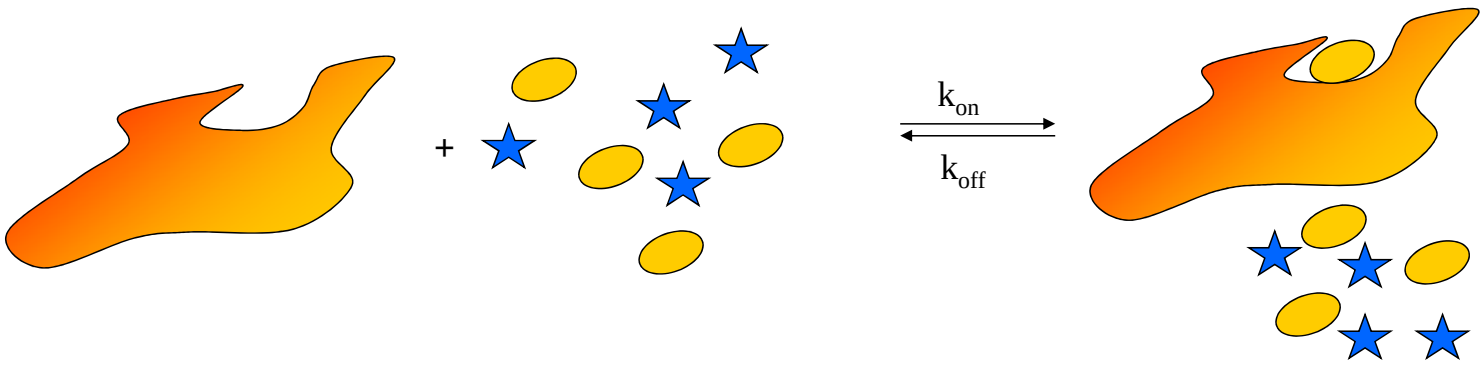

$$Q_{obs} = P_{bound} Q_{bound} + P_{free} Q_{free} + Q_{ex}$$

Dipolar interactions: an intermolecular interaction tool

NOE 1D experiment

Données : J. H. Prestegard

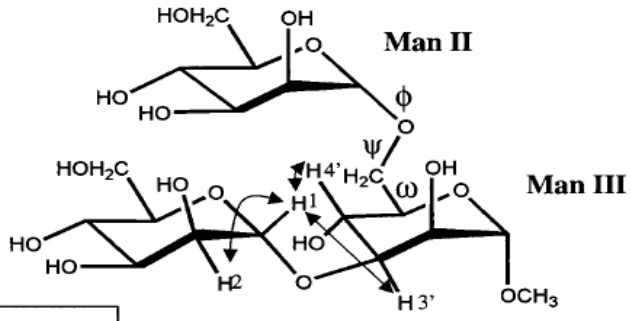

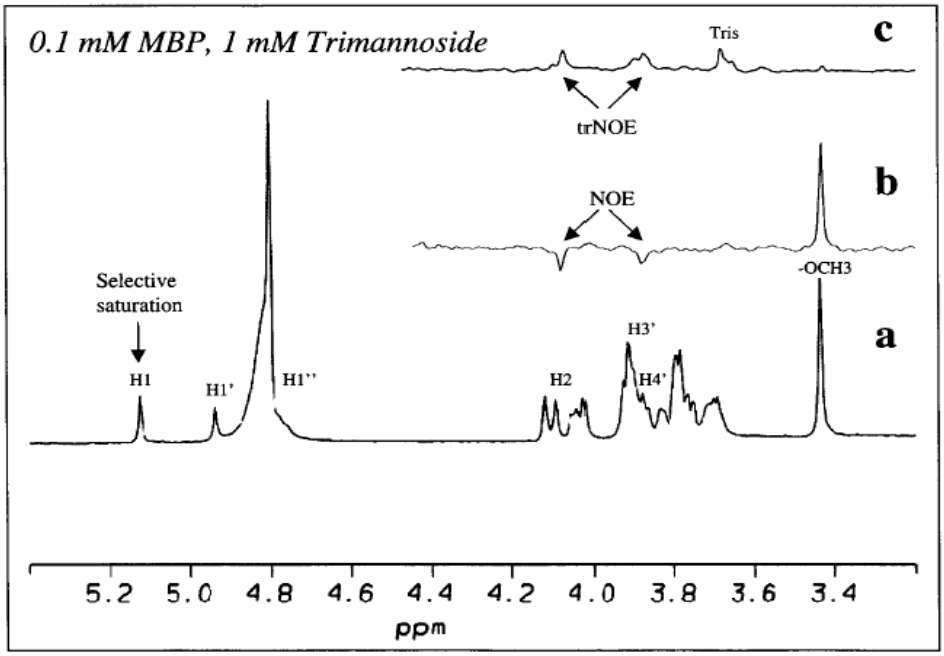

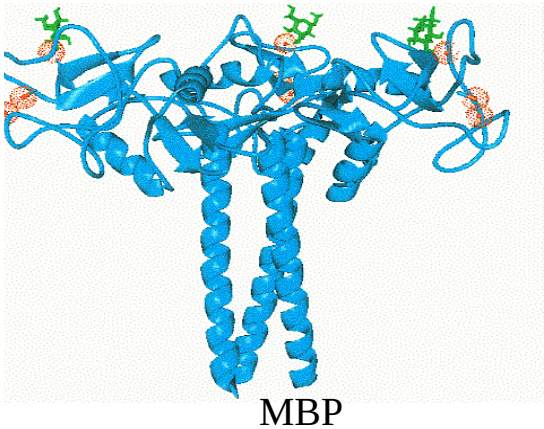

MBP

Dipolar interactions: an intermolecular interaction tool

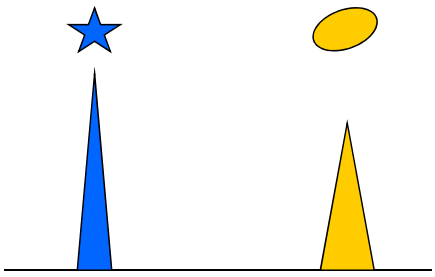

Saturation transfer on free ligand

Saturation

Saturation transfer

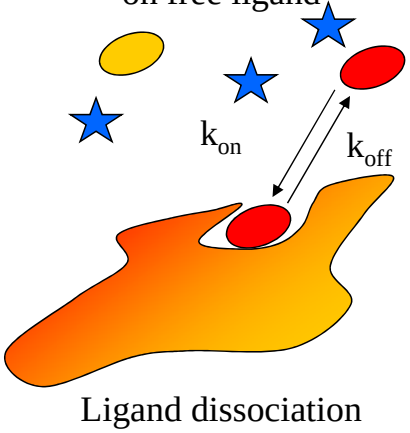

Ligand dissociation

Dipolar interactions: an intermolecular interaction tool

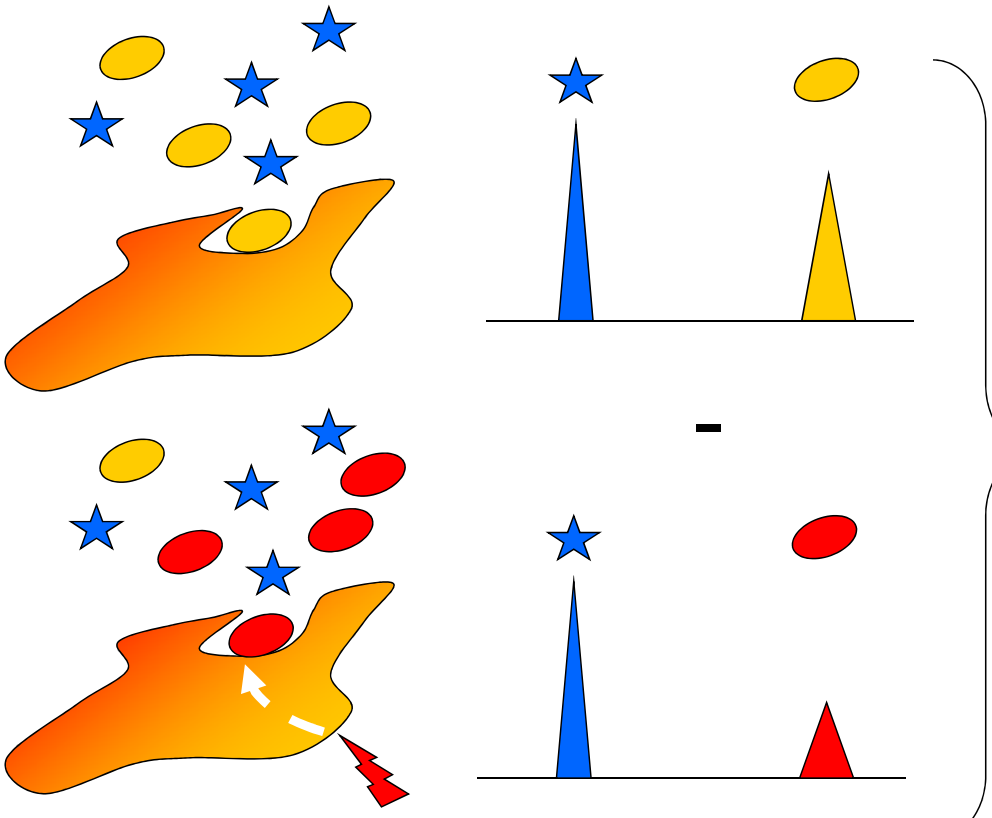

Transfert de saturation invasif

Saturation transfer difference (STD)

Validity of the method:
$10^{-8} < K_D < 10^{-3}$ M

Dipolar interactions: an interaction tool

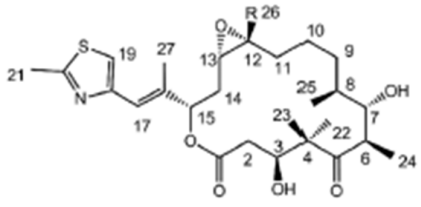

Epothilone A R=H
Epothilone B R=CH_3

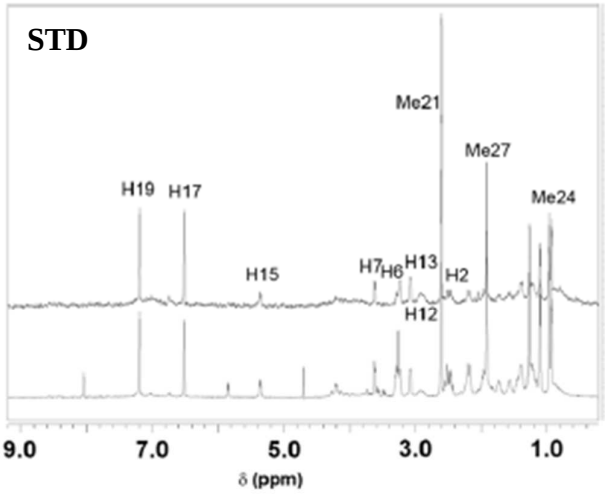

EpoA

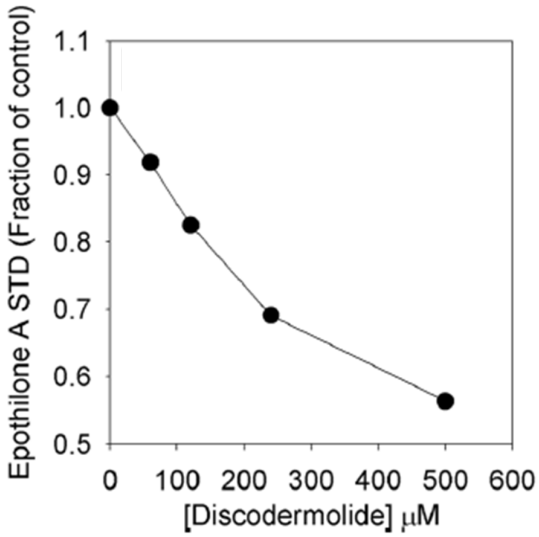

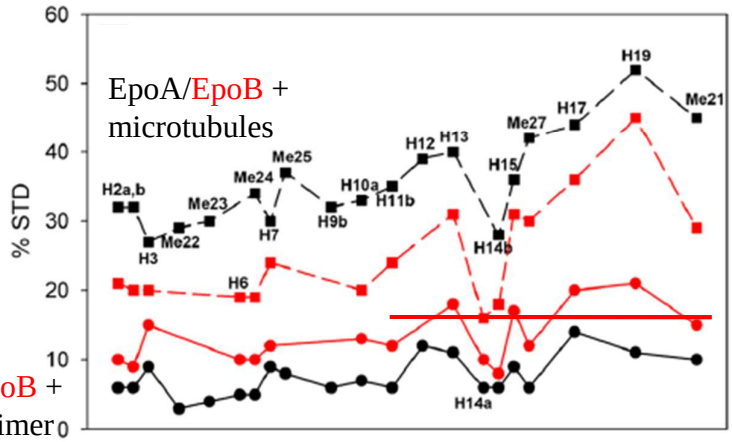

EpoA/EpoB +
tubulin dimer

Dipolar interactions: a dynamical information content

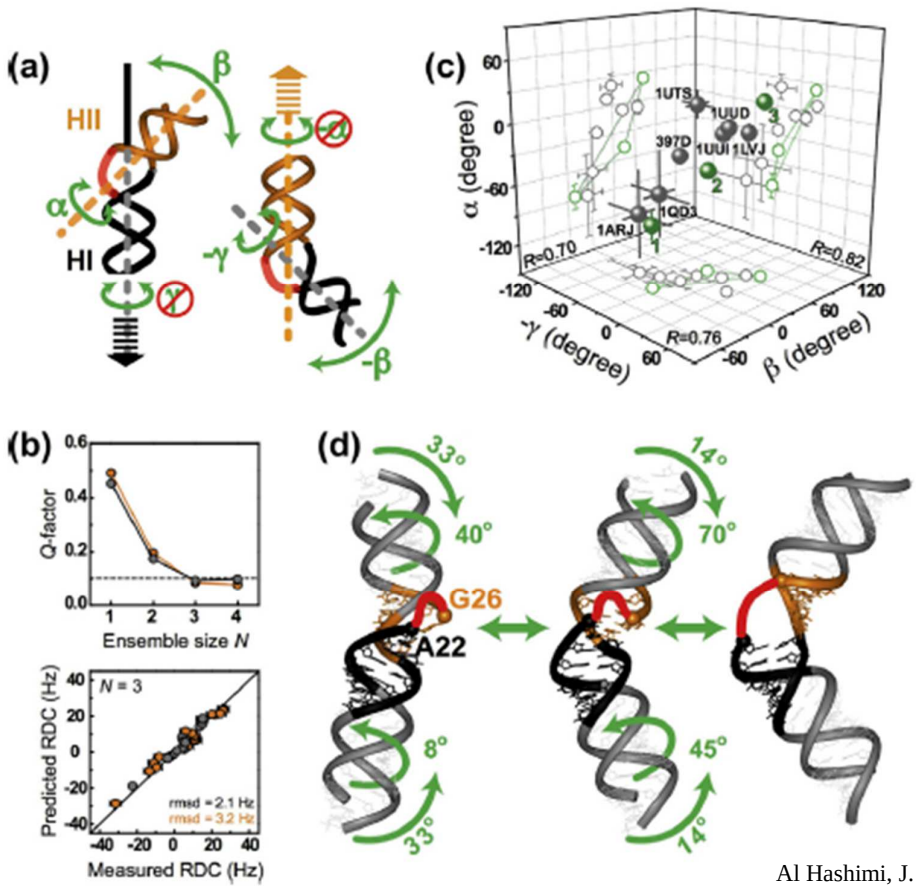

Al Hashimi, J. Magn. Res. **2013**, 191-204

Conclusion

Chemical shift information:

- a structural information content
- a powerful tool to follow local changes; specific interest in functional studies

Relaxation parameters:

- a measure of the dynamics in the ps-ns time-scale; an access to motion
- a tool for interaction studies

Scalar couplings:

- a unique tool to transfer magnetization for the spectroscopist
- an angular information

Dipolar interactions:

- an orientational and distance information
- a source of intermolecular contact information
- a source of dynamical information in the µs-ms time-scale

Conclusion

Structural information
Local probes

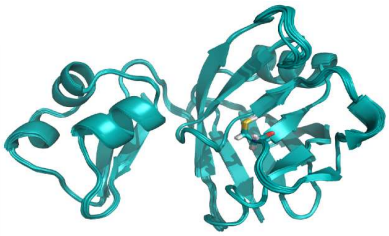

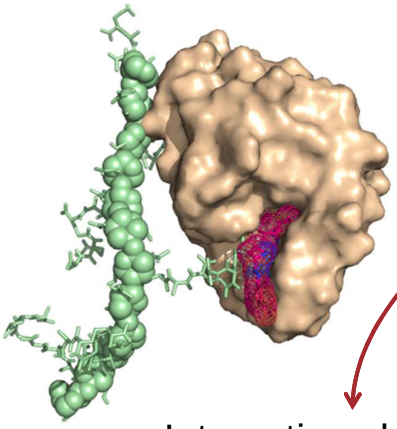

Biomolecular NMR

Dynamical information:
amplitude and
time-scale of motion

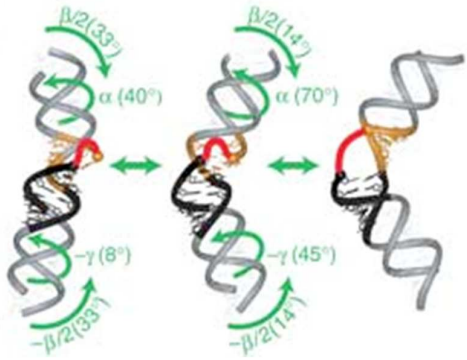

Interactions between
different partner :
interaction site, K_D